FINAL REPORT

High-resolution climate scenarios for basin-scale water resource management applications

Final Report

15.02.2023

Project Title:	High-resolution climate scenarios for basin-scale water resource management applications
Funding Agency:	National Mission for Clean Ganga
Project No.:	TE-16015/2/2019/NMCG

Principal Investigator: Dr. Somnath Baidya Roy

Centre for Atmospheric Sciences

IIT Delhi

CONTENTS

ABSTRACT

Climate change is likely to significantly affect water resources. High-resolution climate and climate change data can be used to drive hydrological models to understand the spatio-temporal variability of water resources and estimate the hazards, vulnerability and risks due to climate change. This proposal aims to develop high-resolution (10 km x 10 km) datasets of current climate and future climate scenarios and demonstrate its applicability for water resource management problems in the Indo-Gangetic Plain.

1. OBJECTIVES

The objectives of this proposal are as follows:

1. Develop a high-resolution (10 km x 10 km) dataset in gridded format of meteorological variables for current and future climate scenarios.
2. Develop a district-scale dataset in Excel format of current and future climate scenarios
3. Demonstrate the applicability of such data for basin-scale water resource management problems under climate change for selected basins in the Indo Gangetic Plains.

2. TASKS

	TASK	**Status**
Task 1	Acquire coarse resolution data for model parameterization, calibration and evaluation	Completed
Task 2	Conduct Test simulations to configure, evaluate, calibrate and improve WRF	Completed
Task 3	Generate gridded downscaled dataset at 10 km resolution for current (2005-2015) and future climate scenarios (RCP4.5 and RCP 8.5 for 2041-2050 and 2091-2100 periods) using WRF driven by coarse-resolution climate data and scenarios from Bruyere et al. (2015). The dataset will consist of meteorological variables such as temperature, humidity, radiation, wind, cloud, precipitation and surface sensible heat	Completed

	flux and evapotranspiration that are used for hydrological modeling.	
Task 4	Generate district scale dataset using GIS tools	Completed
Task 5	Conduct Test simulations for current climate with the VIC model to configure, evaluate and calibrate the VIC model	Completed
Task 6	Conduct simulations with the VIC model over selected basins	Completed

3. RESULTS

3.1 Task 1: Data acquisition

3.1.1 Survey of climate data available over India

3.1.1.1 Historical and present climate:

This project will generate high-resolution climate data for the Indo-Gangetic Plain for water resource applications at basin and district scale. Table 1 below shows the current status of available meteorological data available the covers the entire study area. The datasets include gridded products from station observations from the India Meteorological Department (IMD) and the Global Historical Climatology Network (GHCN) as well as various reanalyses products that are generated by objectively synthesizing numerical model outputs with available observations. The best available option is ERA5 Reanalyses (0.25 degree x 0.25 degree) but even that is inadequate for district-scale applications.

Table 1 : Climate datasets available over Indian region for historical-present day period

	Datasets and references	Type	Spatial resolution	Availability	Shortcomings/ Comments
1	India Meteorological Department (IMD) observations *(Rajeevan et al. 2005, Srivastava et al. 2008)*	Ground station observations	1˚ x 1˚ resolution for gridded data	1951-2018 Daily	• Only temperature and precipitation datasets are gridded for India • Coarse spatial resolution

					• Future scenario uncertain
2	CERA-20C Coupled ocean-atmosphere Reanalysis (ECMWF) *(Laloyaux et al. 2018)*	Reanalysis of 20th century	~125 km	1901-2010 Sub-daily, Daily, Monthly	• Coarse spatial resolution • No data available after 2010
3	Climate Forecast System Reanalysis (NCEP) *(Saha et al. 2010)*	Reanalysis	0.5° x 0.5° and 2.5° x 2.5°	1979-2017 Sub-daily, Monthly	• Coarse spatial resolution • No data available after 2017
4	NCEP/NCAR R1 and R2 *(Kalnay et al. 1996)*	Reanalysis	2.5°x2.5°	1948-present (R1) ,1979-present (R2) Sub-daily, Daily, Monthly	• Coarse spatial resolution
5	NOAA 20th Century Reanalysis (ESRL) *(Compo et al. 2011)*	Reanalysis	2° x 2°	1871-2014 Daily, Monthly	• Coarse spatial resolution • No data available after 2014
6	JRA-55 (Japanese Meteorological Agency) *(Kobayashi et al. 2015)*	Reanalysis	1.125°x 1.125° / 2.5° x 2.5°	1957-present Monthly	• Coarse spatial resolution • Inadequate temporal resolution
7	NASA MERRA2 (Global Modelling and Assimilation Office) *(Molod et al. 2015)*	Reanalysis	½° latitude by ⅝° longitude	1980-2017 Sub-daily, Daily, Monthly	• Coarse spatial resolution • No data available after 2017
8	ERA40 (ECMWF) *(Uppala et al. 2005)*	Reanalysis	1.125°x 1.125° /	1957-2002 Sub-daily, Monthly	• Coarse spatial resolution • No data available after 2010

			2.5° x 2.5°		
9	ERA-Interim (ECMWF) *(Berrisford et al. 2009)*	Reanalysis	0.125˚x 0.125˚	1979-2018 Sub-daily, Daily, Monthly	• RH to be derived from dew point temperature and T2
10	ERA-5 (ECMWF) *(Hersbach, 2016)*	Reanalysis	0.25˚ x 0.25˚	1950-present Sub-daily, Daily, Monthly	• RH to be derived from dew point temperature and T2m
11	Global Ensemble Forecast System Reforecast (ESRL/NOAA) *(Hamill et al. 2013)*	Model forecast	1˚ x 1˚	1984-present with a forecast up to 15 days Sub-daily, Daily	• RH to be derived from Specific humidity • For higher resolution data can be downscaled
12	GHCN (Global Historical Climatology Network) *(Vose et al. 1992)*	Gridded station observation Products –Bias corrected	0.5° x 0.5°	1870-2014 Monthly	• Only temperature and precipitation variables are available • Coarse spatial resolution • No data available after 2014 • Inadequate temporal resolution
13	CESM historical *(Kay et al. 2015)*	Ensemble simulation	1.9° x 2.5°	1850-2005 Daily	• For higher resolution data can be downscaled
14	NCEP FNL/GFS	Model simulation	1˚ x 1˚	1999-present Sub-daily, Daily	• For higher resolution data can be downscaled

3.1.1.2 Future climate scenarios:

Future climate scenarios are generated by General circulation Models (GCM). The Fifth Coupled Model Intercomparison Project (CMIP5, Taylor et al., 2012) maintains a repository of GCM simulations conducted under the project. Table 2 shows the models for which sub-daily scale data is available for different scenarios.

Table 2: Climate datasets available over Indian region for future scenarios

Models	Source	Spatial resolution		Availability	Variables
		Lat	Lon		
MRI-CGCM3	Meteorological Research Institute, Japan Meteorological Agency	1.1214	1.125	2006-2100 3hr, 6hr, daily	Relative Humidity, Daily-Mean Near-Surface Wind Speed, Precipitation, Air Temperature
MIROC5	National Institute for Environmental Studies, Japan Agency for Marine-Earth Science and Technology	1.4008	1.40625	2006-2100 3hr, 6hr, daily	Precipitation flux, Air Temperature, Eastward Near-Surface Wind Speed, Northward Near-Surface Wind Speed, Near-Surface Specific Humidity
MIROC-ESM/ MIROC-ESM-CHEM	Atmosphere and Ocean Research Institute, Japan Agency for Marine-Earth Science and Technology	2.7906	2.8125	2006-2100 3hr, 6hr, daily	Near-Surface Specific Humidity, Precipitation, Air Temperature, Eastward Near-Surface Wind Speed, Northward Near-Surface Wind Speed, Relative Humidity
MRI-ESM1	Meteorological Research Institute, Japan Meteorological Agency	1.1214	1.125	2006-2100 3hr, 6hr, daily	Near-Surface Specific Humidity, Precipitation, Air Temperature, Eastward Near-

					Surface Wind Speed, Northward Near-Surface Wind Speed
ACCESS1.0 /1.3	Centre for Australian Weather and Climate Research	1.25	1.875	2006-2100 6hr, daily	Relative Humidity, Precipitation, Air Temperature, Eastward Near-Surface Wind Speed, Northward Near-Surface Wind Speed
HadGEM2-ES/CC	Met Office Hadley Centre	1.25	1.875	2005-2100 3hr, 6hr, daily	Relative Humidity, Precipitation, Air Temperature, Eastward Near-Surface Wind Speed, Northward Near-Surface Wind Speed
Community Climate System Model 4	National Center for Atmospheric Research	0.9424	1.25	2006-2100 3hr, 6hr, daily	Near-Surface Specific Humidity, Precipitation, Air Temperature, Eastward Wind, Northward Wind
CNRM-CM5	Centre National de Recherches Meteorologiques, Météo-France	1.4008	1.40625	2006-2100 daily	Relative Humidity, Precipitation, Air Temperature, Eastward Near-Surface Wind Speed, Northward Near-Surface Wind Speed
FGOALS-G2.0	Institute of Atmospheric Physics, Chinese Academy of Sciences	2.7906	2.8125	2006-2101 3hr, 6hr, daily	Relative Humidity, Precipitation, Air Temperature, Eastward Wind, Northward Wind
CanESM2	Canadian Centre for Climate Modelling and Analysis, experiment	2.7906	2.8125	2006-2100 6hr, daily	Relative Humidity, Precipitation, Air Temperature, Eastward Near-Surface Wind Speed,

					Northward Near-Surface Wind Speed
CMCC-CM	Centro Euro-Mediterraneo per	1.4008	1.40625	2006-2100 6hr, daily	Relative Humidity, Precipitation, Air Temperature, Eastward Near-Surface Wind Speed, Northward Near-Surface Wind Speed
INM-CM4	Institute for Numerical Mathematics	1.5	2	2006-2101 3hr, 6hr, daily	Relative Humidity, Precipitation, Air Temperature, Eastward Near-Surface Wind Speed, Northward Near-Surface Wind Speed
MPI-ESM-LR	Max Planck Institute for Meteorology	1.8653	1.875	2006-2100 6hr, daily	Relative Humidity, Precipitation, Air Temperature, Eastward Near-Surface Wind Speed, Northward Near-Surface Wind Speed
EC-EARTH consortium	European Network for Earth System Modelling	1.1215	1.125	2006-2100 daily	Relative Humidity, Precipitation, Air Temperature, Eastward Near-Surface Wind Speed, Northward Near-Surface Wind Speed
IPSL-CM5A-MR/LR	Institute Pierre-Simon Laplace	1.2676 (MR) 1.8947 (LR)	2.5 (MR) 3.75 (LR)	2006-2100 3hr, 6hr, daily	Precipitation, Air Temperature, Eastward Near-Surface Wind Speed, Northward Near-Surface Wind Speed
GISS-E2-H	NASA Goddard Institute for Space Studies	2	2.5	2006-2101 6hr, daily 2006-2080	Specific Humidity, Surface Air Pressure, Air Temperature, Eastward Wind, Northward Wind,

				3hr	Near-Surface Relative Humidity, Precipitation
CSIRO-Mk3.6	Commonwealth Scientific and Industrial Research Organization/Queensland Climate Change Centre of Excellence (CSIRO-QCCCE)	1.8653	1.875	2006-2300 daily 2006-2100 daily	Sea Level Pressure, Air Temperature, Eastward Wind, Northward Wind, Relative Humidity, Precipitation
GFDL-ESM2M/ ESM2G	Geophysical Fluid Dynamics Laboratory	2.0225	2.5	2006-2100 3hr, 6hr, daily	Relative Humidity, Precipitation, Air Temperature, Eastward Near-Surface Wind Speed, Northward Near-Surface Wind Speed

3.1.2 Climate datasets used:

As per the above discussion, it is clear that the available climate data are too coarse for our application. Hence, we will downscale the climate data to a higher resolution with the Weather Research and Forecasting (WRF, Skamarock, et al., 2008) where the climate data will be used as initial and boundary conditions. We will use the ensemble simulation output from CESM *(Kay et al. 2015)* model which is available at a resolution of 1.9° x 2.5° from 2005-2100 onwards. This particular model output data is selected because this data has been bias corrected data using ERA INTERIM as well as converted into an intermediate format compatible with WRF according to the method mentioned in *Bruyère et al. 2014.* This bias correction is required to eliminate the regional- scale biases occurring due to the coarse resolution and the limited representation of some physical processes *(Bruyère et al. 2015)*.

The historical CESM run stops at 2005. So, to simulate current conditions, we will use RCP8.5 scenario runs for 2011-2020. This is the best proxy for the current situation because the observed atmospheric CO_2 forcing follows this scenario. Moreover, the simulated values for the RCP8.5 scenario are a better match with observations than the other scenarios (Fig. 1, Table 3).

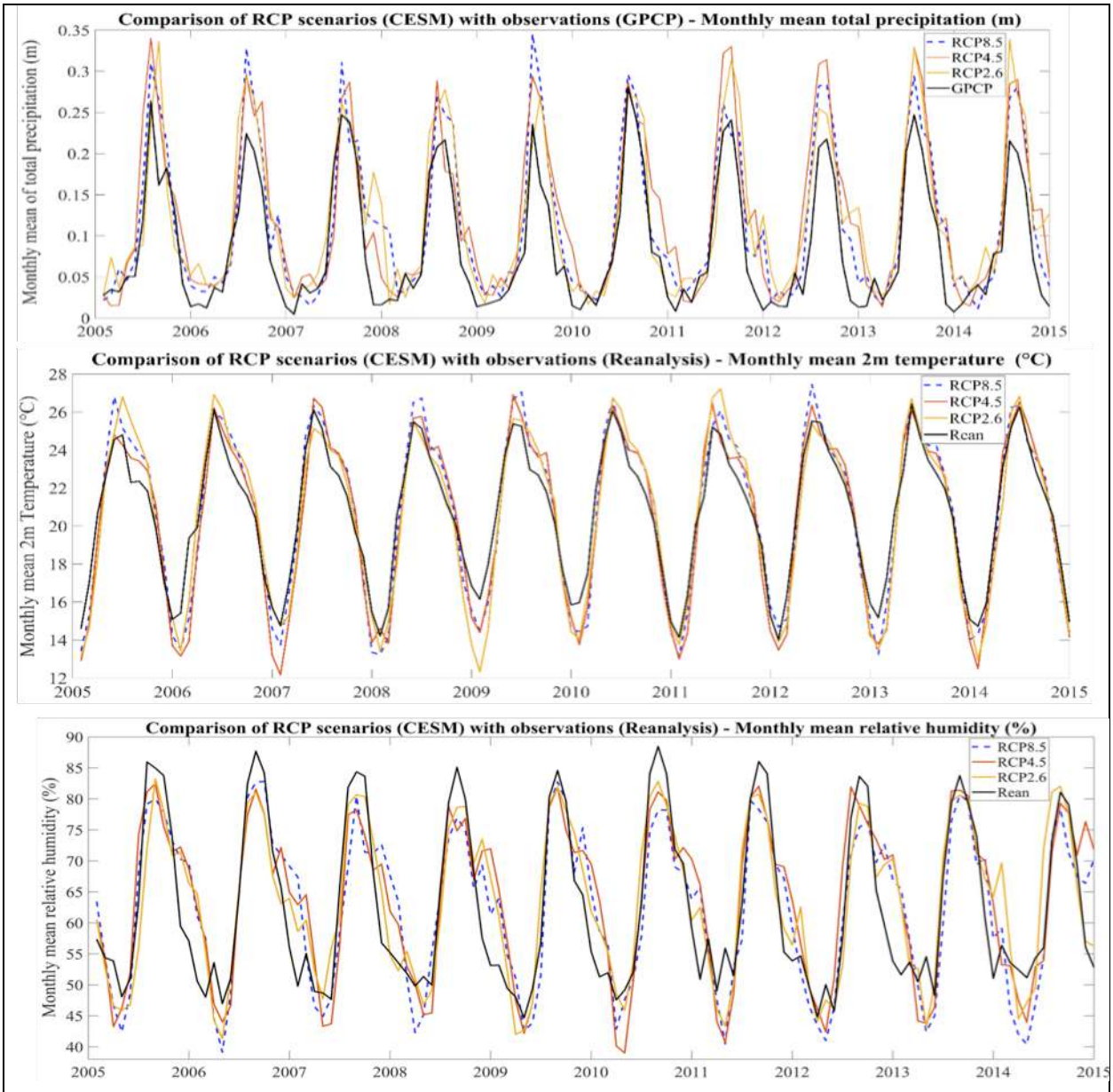

Fig. 1: Comparison of RCP scenarios with observations

Table 3: Comparison of RCP scenarios with observations				
Variable		**RCP8.5**	**RCP4.5**	**RCP2.6**
2m Temperature	Correlation	0.98	0.97	0.96
	Std. Dev	3.94	3.98	3.96
Relative Humidity	Correlation	0.83	0.83	0.88
	Std. Dev	12.89	12.99	12.79

Precipitation	Correlation	0.92	0.90	0.89
	Std. Dev	1.03	1.08	1.04

Initial and boundary condition data for WRF sensitivity simulations and ERA5 data for WRF model evaluation have been acquired.

3.1.3 Preliminary analysis of effect of climate change on Ganga Basin

A preliminary analysis was conducted to estimate the possible impacts of climate change on the Ganga Basin using the CMIP5 multimodel mean outputs for current and historical periods. The results are shown in figures 2-5 that depict the RCP8.5 end century (2091-2100 average) and current (2001-2010) scenarios and the difference between them for 2m temperature (Fig. 2), precipitation (Fig. 3), near surface relative humidity (Fig. 4), and surface evapotranspiration (Fig. 5).

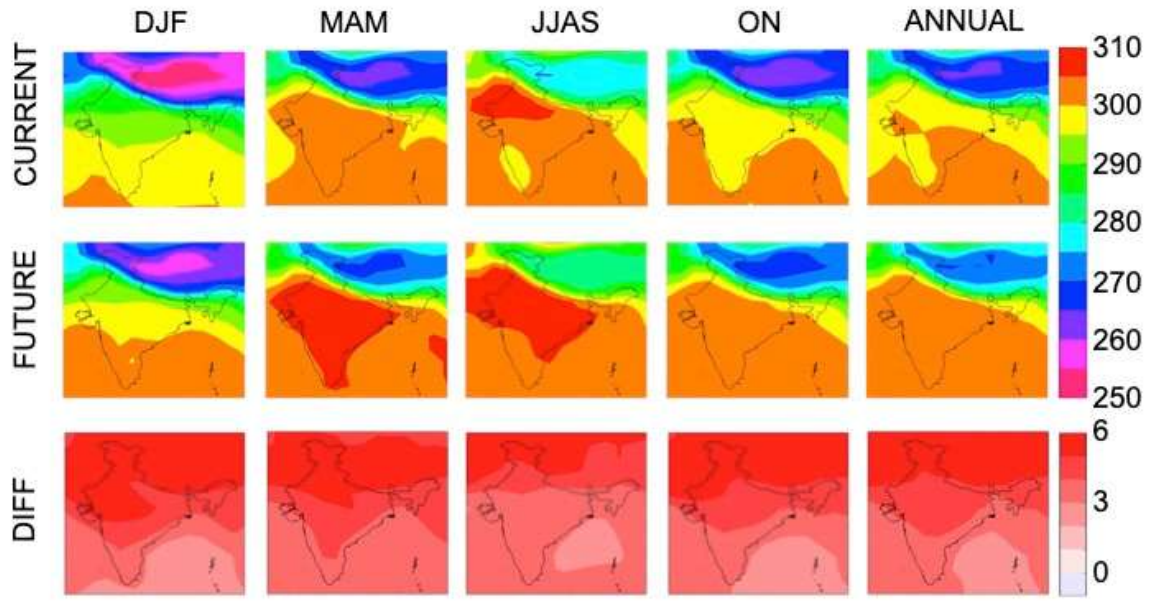

Figure 2: Current (2001-2010) and Future end-century (2091-2100) RCP8.5 scenarios for 2m Temperature (K) and the difference between them averaged for winter (DJF), spring (MAM), monsoon (JJAS), autumn (ON) and the whole year. For the difference plots, only the grid cells that are statistically significant at p<0.05 using the Wilcoxon Sign Rank test are shown.

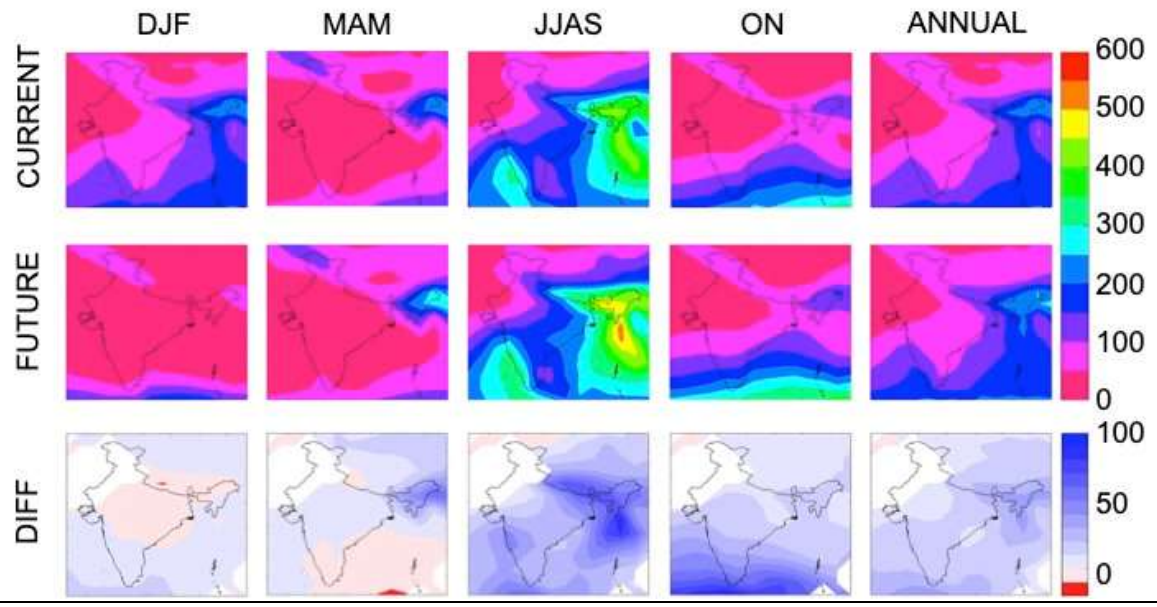

Figure 3: Current (2001-2010) and Future end-century (2091-2100) RCP8.5 scenarios for accumulated precipitation (mm/month) and the difference between them averaged for winter (DJF), spring (MAM), monsoon (JJAS), autumn (ON) and the whole year. For the difference plots, only the grid cells that are statistically significant at p<0.05 using the Wilcoxon Sign Rank test are shown.

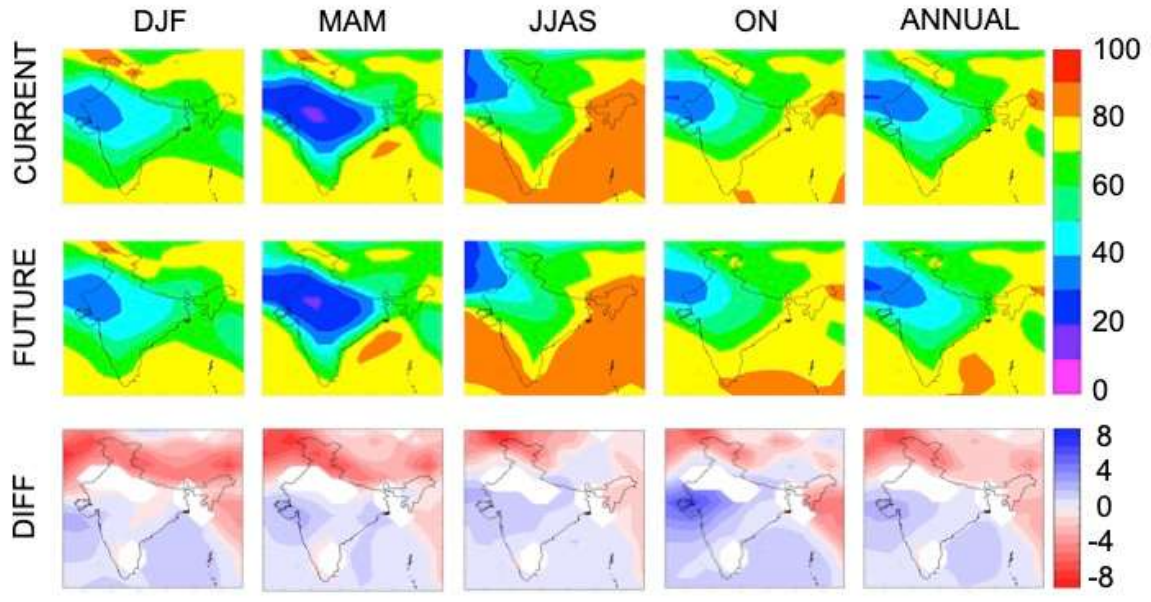

Figure 4: Current (2001-2010) and Future end-century (2091-2100) RCP8.5 scenarios for rear surface relative humidty (%) and the difference between them averaged for winter (DJF), spring (MAM), monsoon (JJAS), autumn (ON) and the whole year. For the difference plots, only the grid cells that are statistically significant at p<0.05 using the Wilcoxon Sign Rank test are shown.

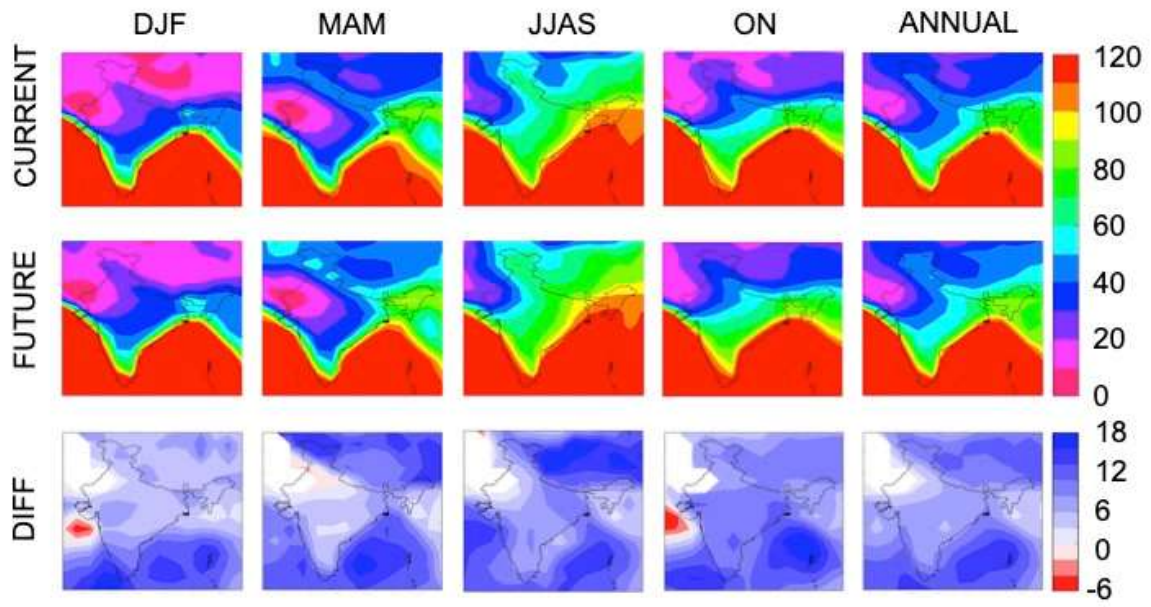

Figure 5: Current (2001-2010) and Future end-century (2091-2100) RCP8.5 scenarios for surface evapotranspiration (mm/month) and the difference between them averaged for winter (DJF), spring (MAM), monsoon (JJAS), autumn (ON) and the whole year. For the difference plots, only the grid cells that are statistically significant at p<0.05 using the Wilcoxon Sign Rank test are shown.

Results show that climate change is likely to increase 2m temperatures by 2-5 degrees across all seasons, increase precipitation by up to 20 mm/month during the monsoon season, and increase ET by up to 10 mm during the monsoon and autumn seasons. The relative humidity will not show a lot of changes because, even though the moisture content of the air will increase, the moisture holding capacity of the air will also increase due to the warming.

These changes are likely to have a strong effect on the hydrology of the Ganga basin.

3.2 Task 2: Sensitivity simulations

3.2.1 Literature review:

Earlier studies have tested many different configurations of WRF and identified the best possible combination for their study domain. Literature review was conducted to study these configurations used in earlier work for simulations similar in resolution to those planned for this project. A comparison of the configurations including shortwave (SW) and Longwave (LW) radiations, Planetary Boundary Layer (PBL) and cumulus convection schemes is given in Table 4 below.

Table 4: Physics schemes used in WRF simulations for comparable cases						
	R1	R2	R3	R4	R5	R6
Shortwave Radiation	cam schemes	cam schemes	cam schemes		cam schemes	Dudhia scheme
Longwave Radiation	cam schemes	cam schemes	cam schemes		cam schemes	rrtm scheme
Land surface phyiscs	Noah scheme	Noah scheme	CLM4/10-layer	Noah scheme	Noah scheme	Noah scheme
Surface layer physics		MM5 Monin-Obukhov scheme		Revised MM5 scheme (Jimenez)		
PBL	Mellor-Yamada-Janjic TKE scheme	YSU scheme	YSU scheme	UW boundary layer scheme from CAM5	YSU scheme	YSU scheme
Microphysics	Thompson scheme	WSM 3-class simple ice scheme	WSM 6-class graupel scheme	WDM 6-class scheme	WSM 6-class graupel scheme	WSM 6-class graupel scheme
Cumulus physics	Betts-Miller-Janjic scheme	Kain-Fritsch (new Eta) scheme	New GFS simplified Arakawa-Schubert scheme from YSU	Betts-Miller-Janjic scheme	Kain-Fritsch (new Eta) scheme	Kain-Fritsch (new Eta) scheme
Resolution	20*20km	30km and 10km	4km and 25km	10km	30km	27, 9, 3 and 1km

	R7	R8	R9	R10	R11	R12
Shortwave Radiation	Dudhia scheme	rrtmg scheme	rrtmg scheme	Dudhia scheme	Dudhia scheme	MM5 shortwave
Longwave Radiation	rrtm scheme	rrtmg scheme	rrtmg scheme	rrtm scheme	rrtm scheme	rrtm scheme
Land surface physics	Noah scheme	Noah scheme	Noah scheme	thermal diffusion scheme	Noah scheme	Noah scheme
Surface layer physics			MM5 Monin-Obukhov scheme		MM5 Monin-Obukhov scheme	MM5 Monin-Obukhov scheme
PBL	Bougeault and Lacarrere (BouLac) PBL	YSU scheme	MYNN 2.5 level TKE scheme	YSU scheme	Mellor-Yamada-Janjic TKE scheme	YSU scheme
Microphysics	WSM 5-class scheme	WSM 6-class graupel scheme	Goddard GCE scheme	WSM 3-class simple ice scheme	Goddard GCE scheme	WSM 5-class scheme
Cumulus physics	Kain-Fritsch (new Eta) scheme		Betts-Miller-Janjic scheme	Betts-Miller-Janjic scheme	Betts-Miller-Janjic scheme	Kain-Fritsch (new Eta) scheme
Resolution	30km and 6km	30km, 10km and 2 km	27 and 3 km	30km	27, 9 and 3 km	48, 12 and 4 km
	R13	R14(t2m)	R15	R16	R17	R18

Shortwave Radiation	Dudhia scheme	GFDL	Dudhia scheme	Dudhia scheme	Dudhia scheme	Dudhia scheme
Longwave Radiation	rrtm scheme	GFDL	rrtm scheme	rrtm scheme	rrtm scheme	rrtm scheme
Land surface physics	Noah scheme	Noah scheme	Noah scheme	Noah scheme	Noah scheme	RUC land-surface model
Surface layer physics			MM5 Monin-Obukhov scheme			
PBL	YSU scheme	Mellor-Yamada-Janjic TKE scheme	YSU scheme	YSU scheme	Mellor-Yamada-Janjic TKE scheme	YSU scheme
Microphysics	WSM 3-class simple ice scheme	WSM 6-class graupel scheme for T2m and Thompson scheme for precip	WSM 5-class scheme	WSM 6-class graupel scheme	WSM 3-class simple ice scheme	Thompson scheme
Cumulus physics	Betts-Miller-Janjic scheme	Grell-Devenyi ensemble scheme			Kain-Fritsch (new Eta) scheme	Kain-Fritsch (new Eta) scheme
Resolution	27km	12km	10km and 5km	4km and 1.33km	36km	12km

Summary

The schemes that have been used are summarized as follows in Table 5:

Table 5: Summary of physics schemes used in WRF simulations for comparable cases	
Shortwave Radiation	Dudhia (9), Cam (4), RRTMG (2), MM5 (1), GFDL (1), Goddard (1)
Longwave Radiation	RRTM (10), Cam (4), RRTMG (2), GFDL (1), Goddard (1)
Land surface phyiscs	Noah (16), CLM (1), Thermal diff (1), RUC (1)
Surface layer physics	MM5 MO (5), Revised MM5 (1)
PBL	YSU (11), Mellor-Yamada-Janjic TKE (5), MYNN (1), UW (1), BouLac (1)
Microphysics	WSM6 (6), WSM3 (4), Thompson (3), WSM5 (3), Goddard (2), WDM6 (1)
Cumulus physics	Kain Frtisch (7), Betts-Miller-Janjic (6), Grell-Dev (2), GFS (1)

3.2.2 Model configuration:

3.2.2.1 Domain

The simulations were conducted over a 3700 km x 3700 km domain discretized with a 10 km grid in the horizontal. This grid was nested within two coarser grids with 30 km and 90 km grid spacings and 7050 km x 7050 km and 14130 km x 14130 km sizes, respectively. The domains are shown in Figure 6.

3.2.2.2 Simulation period

The simulations were conducted for the months of January (dry season) and July (wet season) for 2006 (normal), 2007 (wet) and 2009 (dry) years.

3.2.2.3 Initial and Boundary conditions

Initial and lateral boundary conditions for the simulations were obtained from the CESM RCP8.5 projections that show the best match with the observations of emissions and meteorology as discussed in Section 3.1.2.

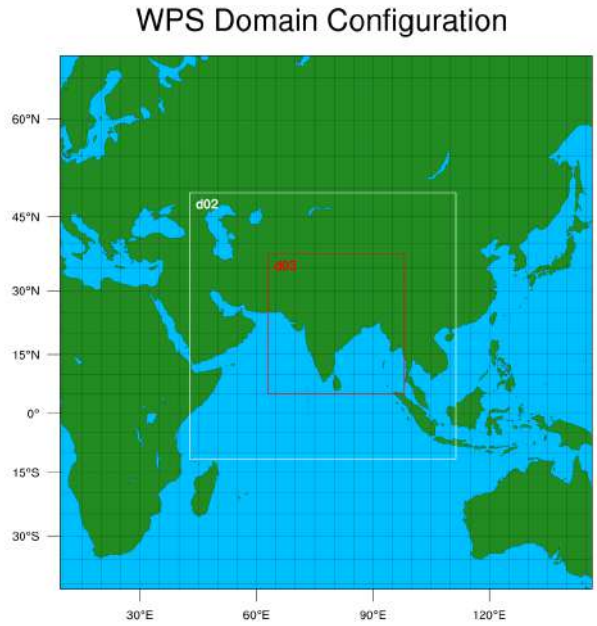

Figure 6: WRF simulation domains showing the 3 nested grids d01, d02 and d03. The results from d03 are used for our analysis

Typically, WRF downscaling simulations are conducted by initializing the model and running it continuously for the desired time period while supplying boundary conditions from coarse-resolution reanalyses or GCM projections. Recent studies including our own (Xia et al., 2017) show that such continuous runs can lead to model drift because WRF is not designed for simulations longer than synoptic timescales. Hence, each test simulations was repeated by reinitializing the model for each day. In other words, each month of the reinitialized simulation is a combination of 30 1-day long simulations.

3.2.2.4 Physics parameterization schemes:

Based on the above literature survey, the following configuration was selected with options for further testing depending on the performance.

- Shortwave radiation scheme: Dudhia
- Longwave radiation scheme: RRTM
- Land surface scheme: NOAH-MP
- Surface layer scheme: MM5
- Planetary Boundary Layer scheme: YSU andMYJ
- Microphysics scheme: WSM6 and Thompson

- Cumulus scheme: BMJ and KF

The experiments with the 8 physics combinations are given in Table 6 below:

Table 6: Physics combinations for sensitivity studies			
S.No.	PBL scheme	Microphysics scheme	Cumulus Scheme
1	YSU	WSM6	BMJ
2	YSU	WSM6	KF
3	YSU	Thompson	BMJ
4	YSU	Thompson	KF
7	MYJ	WSM6	BMJ
8	MYJ	WSM6	KF
9	MYJ	Thompson	BMJ
10	MYJ	Thompson	KF

3.2.2.5 Experiment design

Number of physics combinations: 2 PBL x 2 MP x 2 Cumulus = 8

Number of months of simulations: 2 months per year x 3 years = 6

Types of runs continuos + reinitialized = 2

Total number of simulations: 8 x 6 x 2 = 96

3.2.3 Results

Selected results of the sensitivity studies are presented in figures 7-14. The figures depict monthly mean 2m temperature or monthly accumulated precipitation from the 8 physics combinations along with observations from ERA reanalyses and IMD gridded observations.

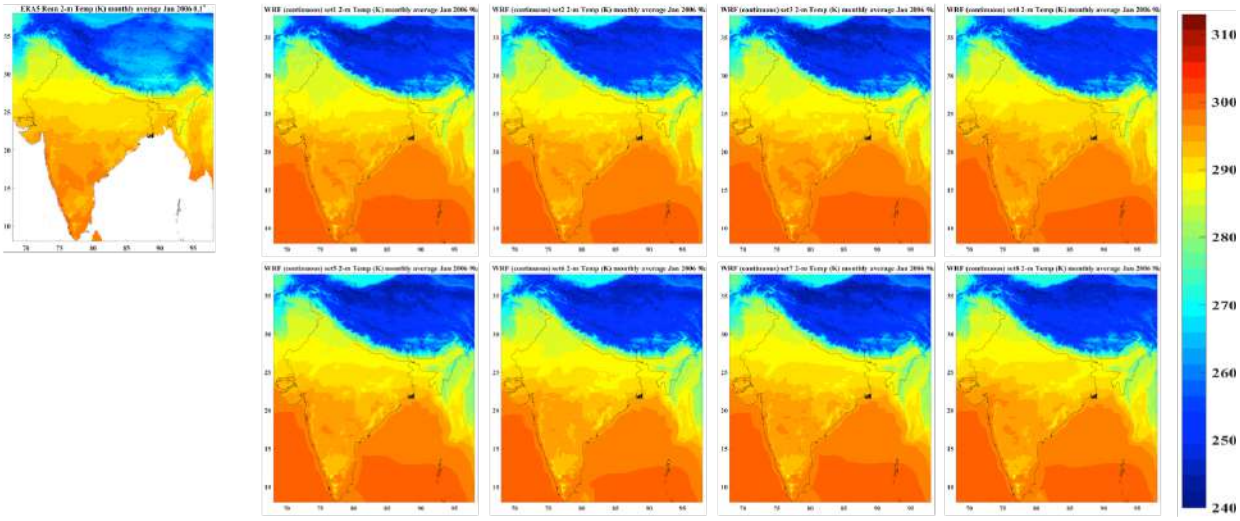

Figure 7: Monthly mean 2m temperature for January 2006 from ERA5 Reanalyses and 8 physics combinations for continuous WRF simulations

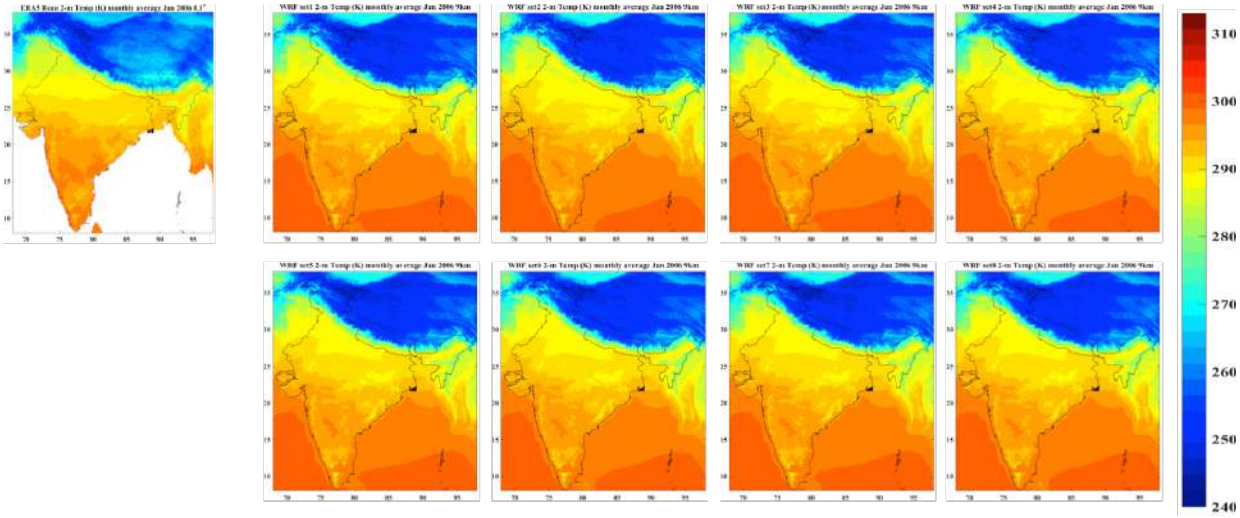

Figure 8: Monthly mean 2m temperature for January 2006 from ERA5 Reanalyses and 8 physics combinations for reinitialized WRF simulations

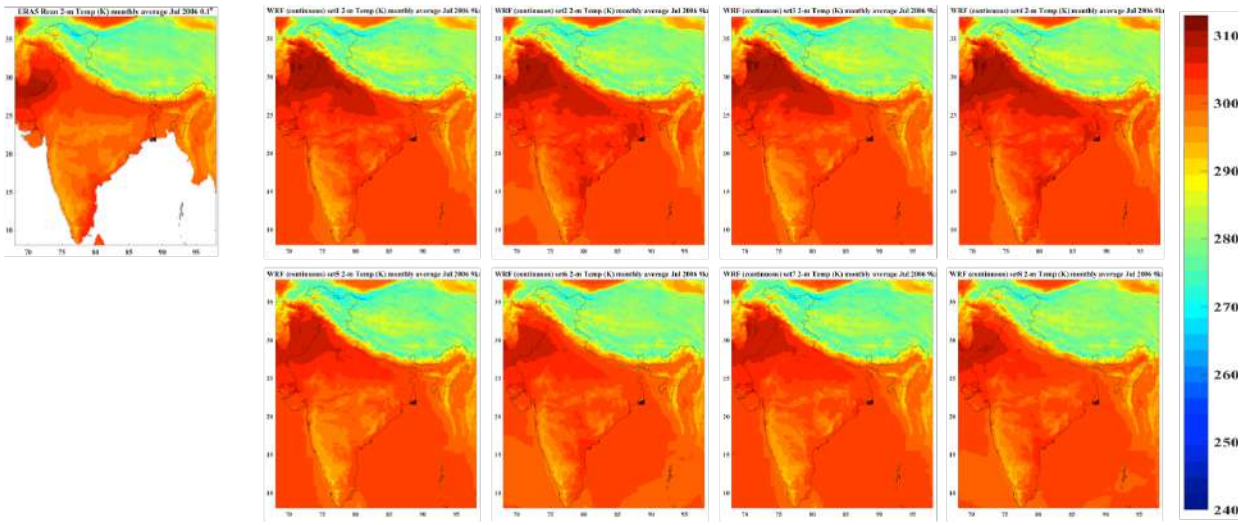

Figure 9: Monthly mean 2m temperature for July 2006 from ERA5 Reanalyses and 8 physics combinations for continuous WRF simulations

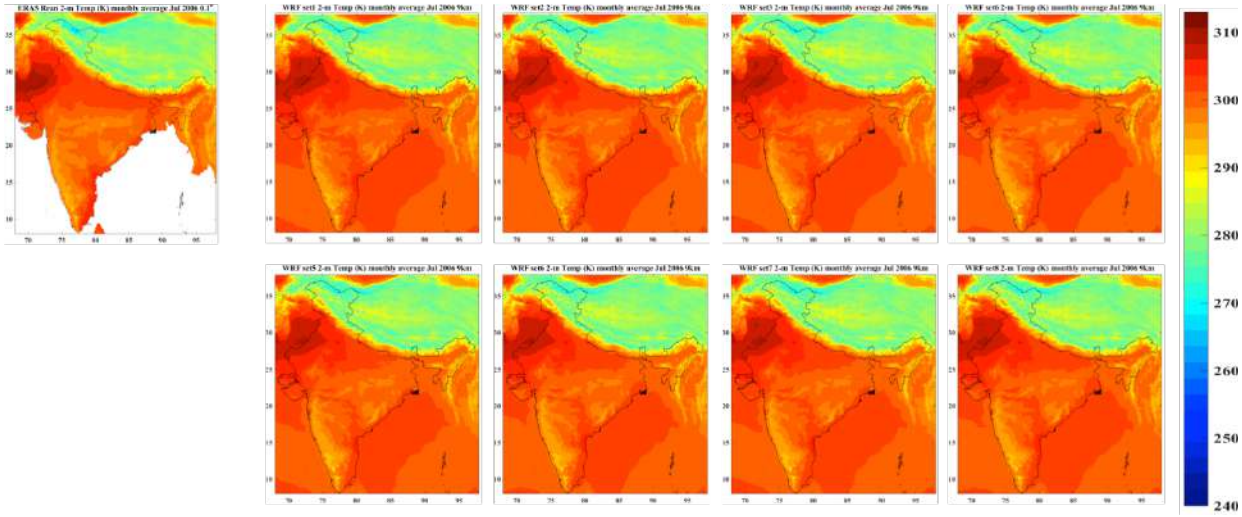

Figure 10: Monthly mean 2m temperature for July 2006 from ERA5 Reanalyses and 8 physics combinations for reinitialized WRF simulations

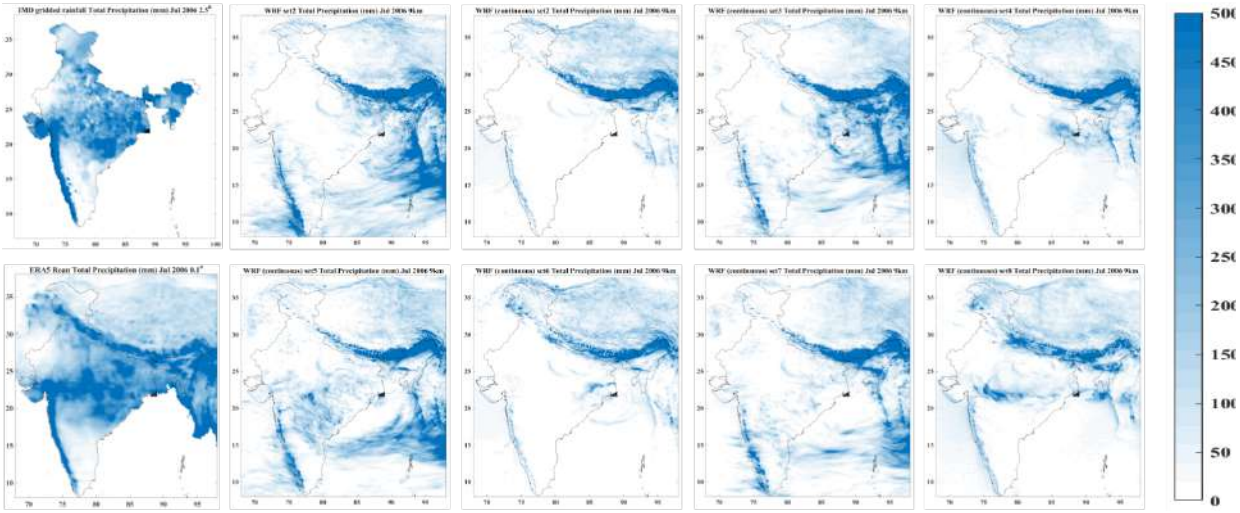

Figure 11: Monthly accumulated precipitation for July 2006 from IMD observations, ERA5 Reanalyses, and 8 physics combinations for continuous WRF simulations

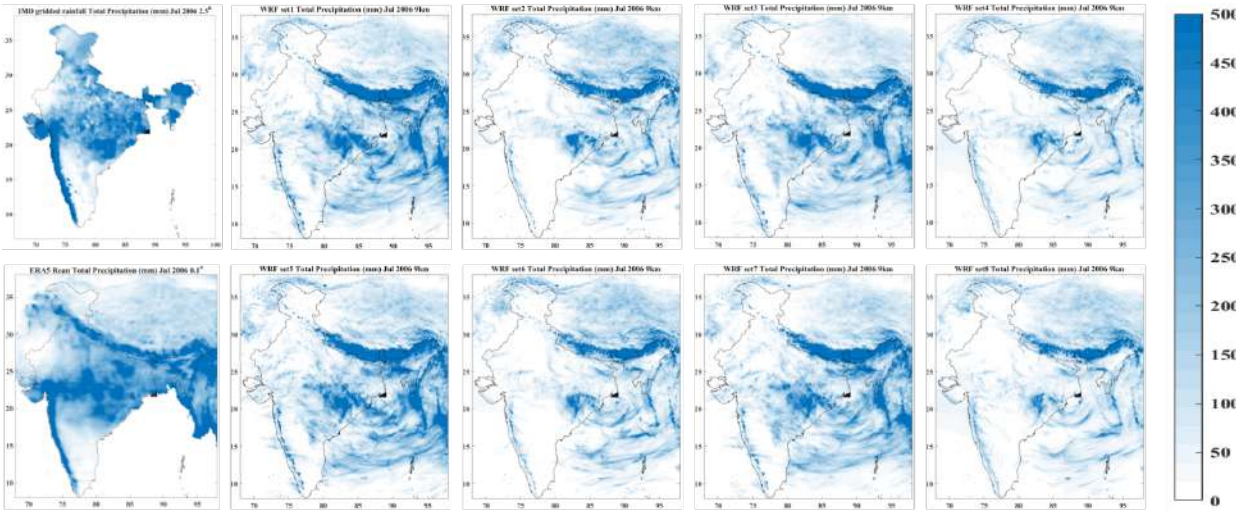

Figure 12: Monthly accumulated precipitation for July 2006 from IMD observations, ERA5 Reanalyses, and 8 physics combinations for reinitialized WRF simulations

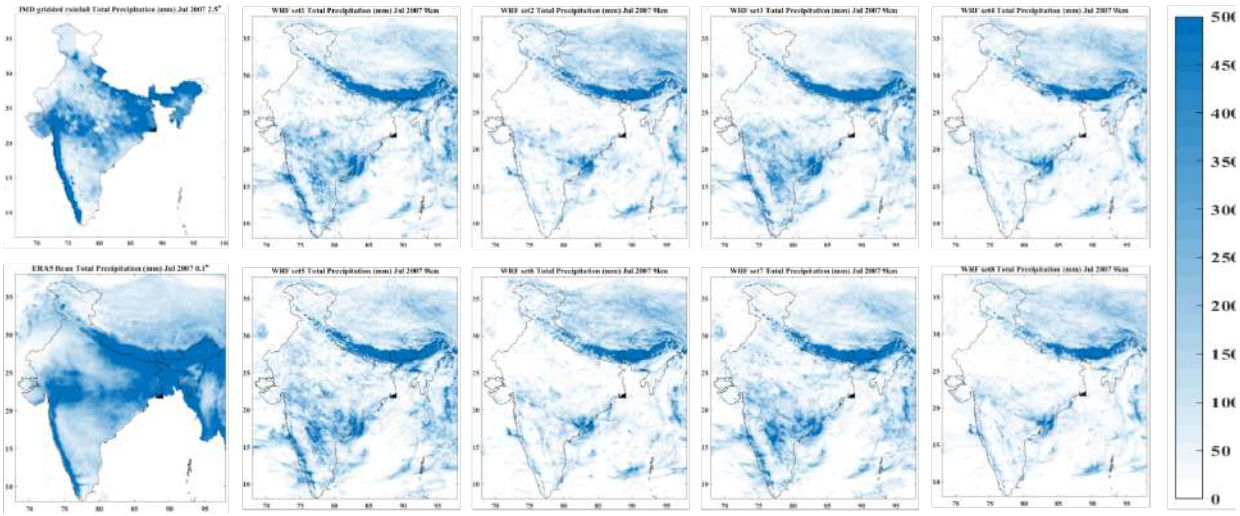

Figure 13: Monthly accumulated precipitation for July 2007 from IMD observations, ERA5 Reanalyses, and 8 physics combinations for reinitialized WRF simulations

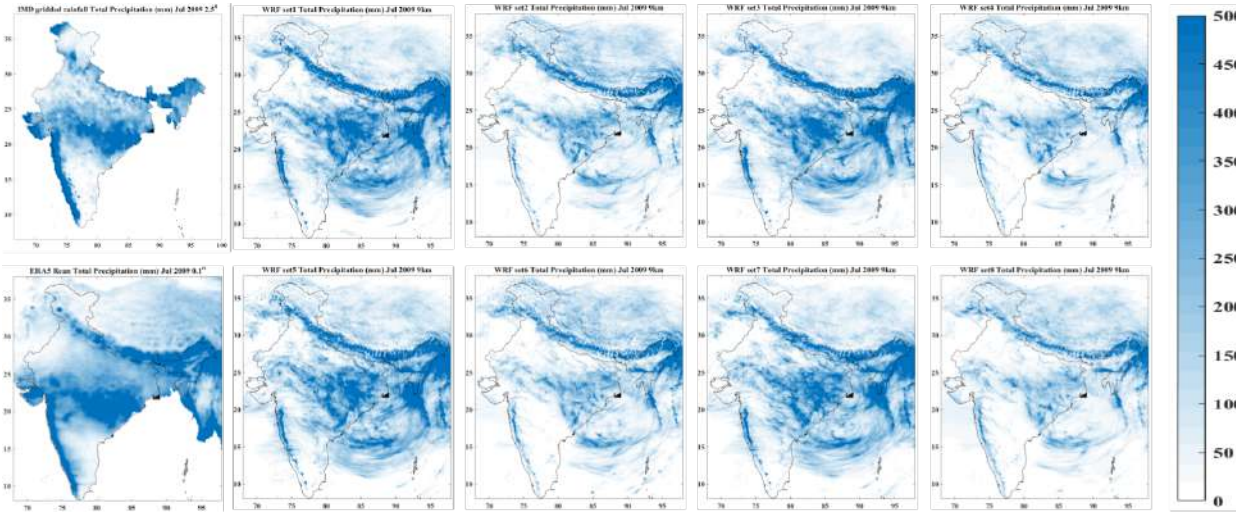

Figure 14: Monthly accumulated precipitation for July 2009 from IMD observations, ERA5 Reanalyses, and 8 physics combinations for reinitialized WRF simulations

3.2.4 Selected configuration

Based on the sensitivity study, we have chosen the continuous approach because the reinitialized simulations are computationally expensive but do not provide any significant advantage over continuous simulations. Furthermore, we have selected the YSU PBL scheme, the KF cumulus scheme, and the WSM6 microphysics scheme for our downscaling simulations.

3.3 Task 3: 10 km gridded downscaled projections

3.3.1 Methods:

With the selected configuration, the WRF model was run one month at a time for the following two periods:

- Current scenario: 2006-2015
- Mid-century RCP8.5 scenario: 2041-2050
- End-century RCP8.5 scenario: 2091-2100

For these runs, we used bias-corrected CESM outputs for the corresponding period as boundary conditions. Because CMIP5 historical scenario was for the 1996-2005 period, for our current scenario runs we used RCP8.5 scenario as the boundary conditions because this scenario is the closest to reality (Fig. 1). The outputs of the simulations were aggregated into time-series and climatology for analysis and dissemination.

3.3.2 Results

Here we present a brief seasonal-scale analysis of the current and future scenarios for temperature and precipitation. The seasons represented are summer (March-May), monsoon (June-September), post-monsoon (October-November), and winter (December-February). The seasonal climatology is constructed by averaging the seasonal data the 10-year period. The seasonal climatology and predicted changes by the end of the century are shown below.

Results show that the Ganga Basin will experience a severe increase in temperatures (Fig. 15) by up to 5 °C and this increase is statistically significant at 99% level (Fig. 23) . The precipitation signal is mixed with almost no change during the winter and summer months. There may be some increase in precipitation by up to 100 mm/month during the monsoon, but this increase is statistically significant only in a small area over Uttar Pradesh (Fig. 24). The post-monsoon season is likely to see a significant increase in precipitation by up to 50 mm. Overall, this indicates that even though climate change may not affect the monsoon precipitation, it may lead to an extension of the monsoon season beyond September.

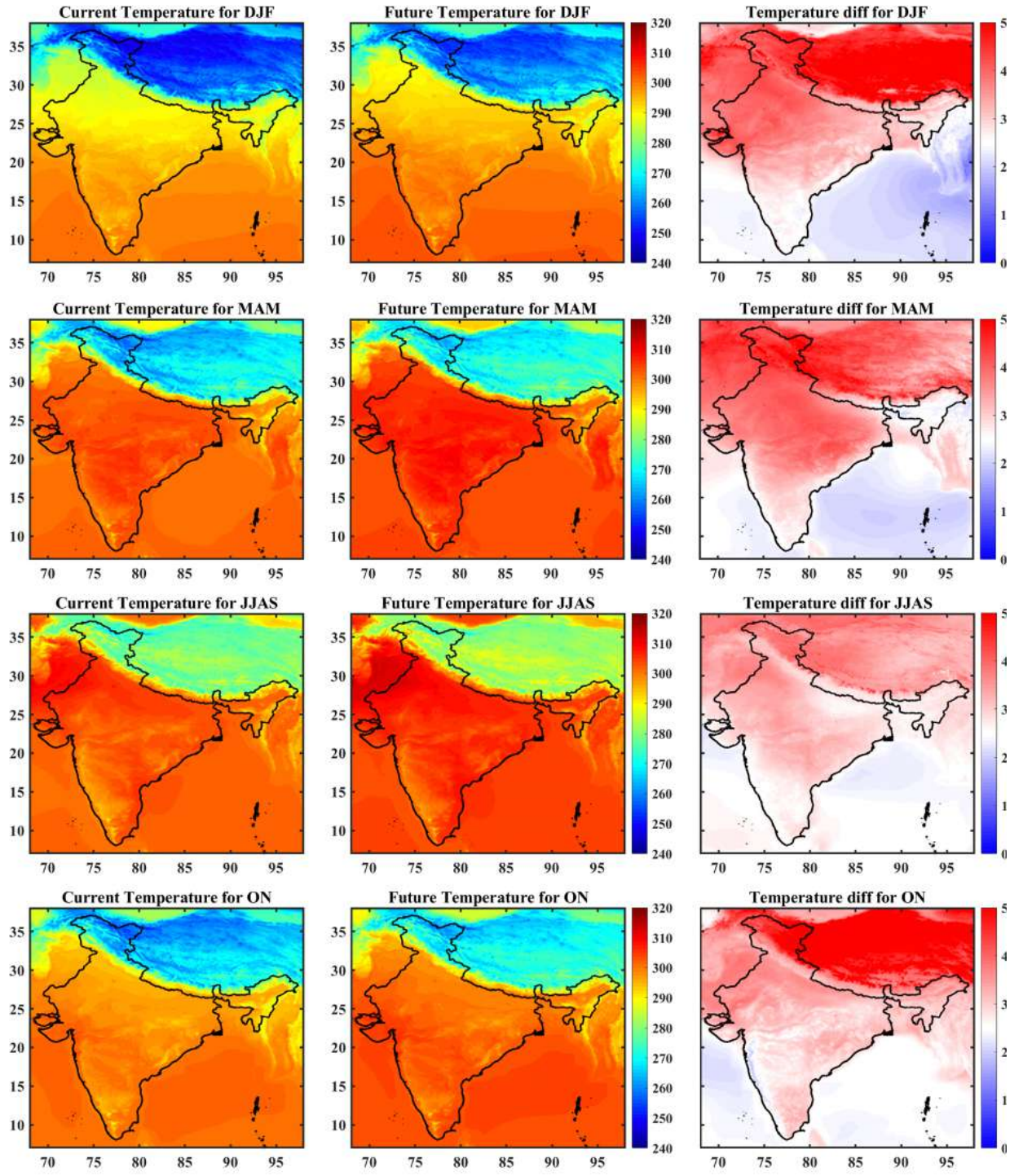

Figure 15: Change in daily mean 2m temperature (°C)

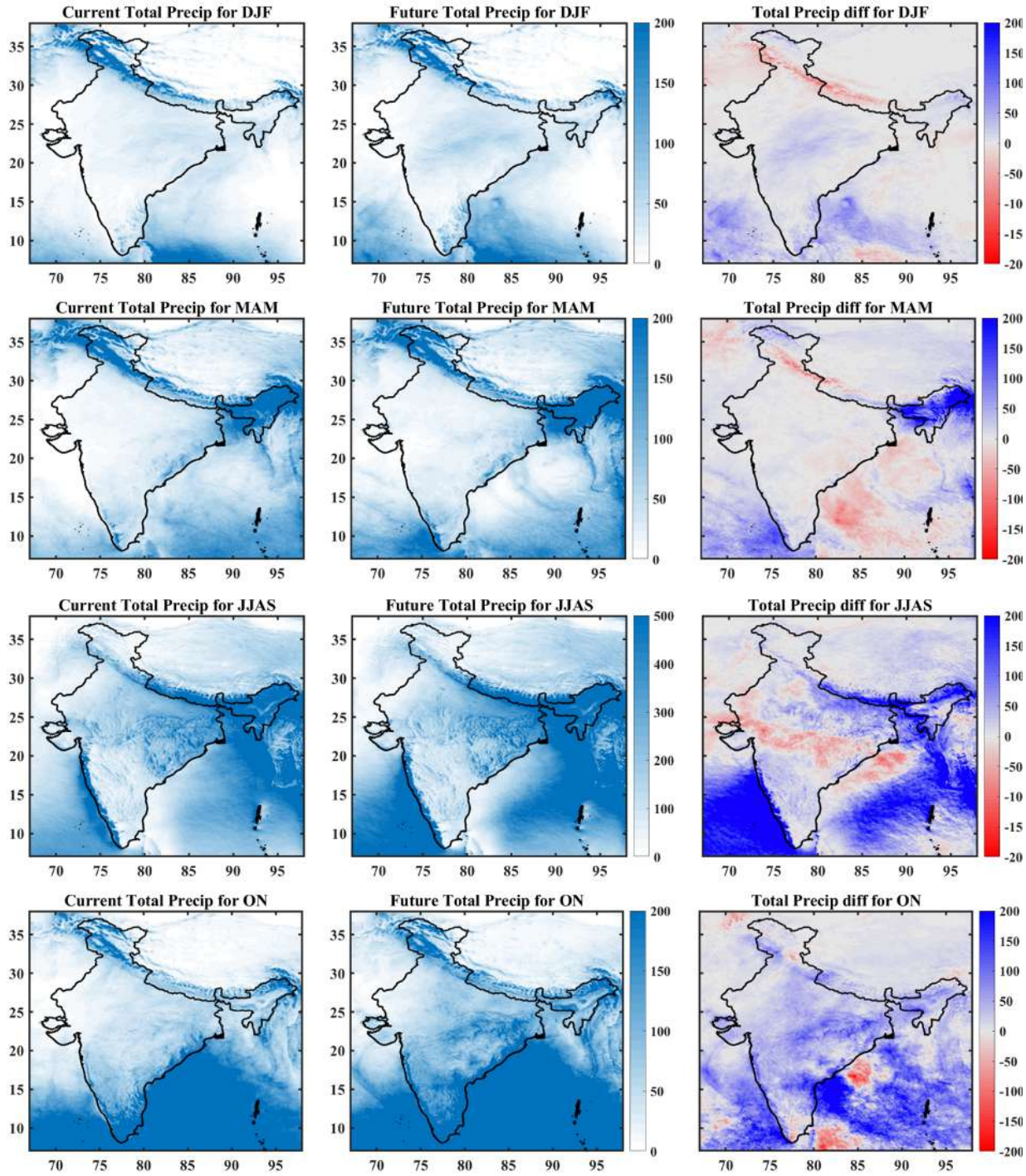

Figure 16: Change in monthly total precipitation (mm/month)

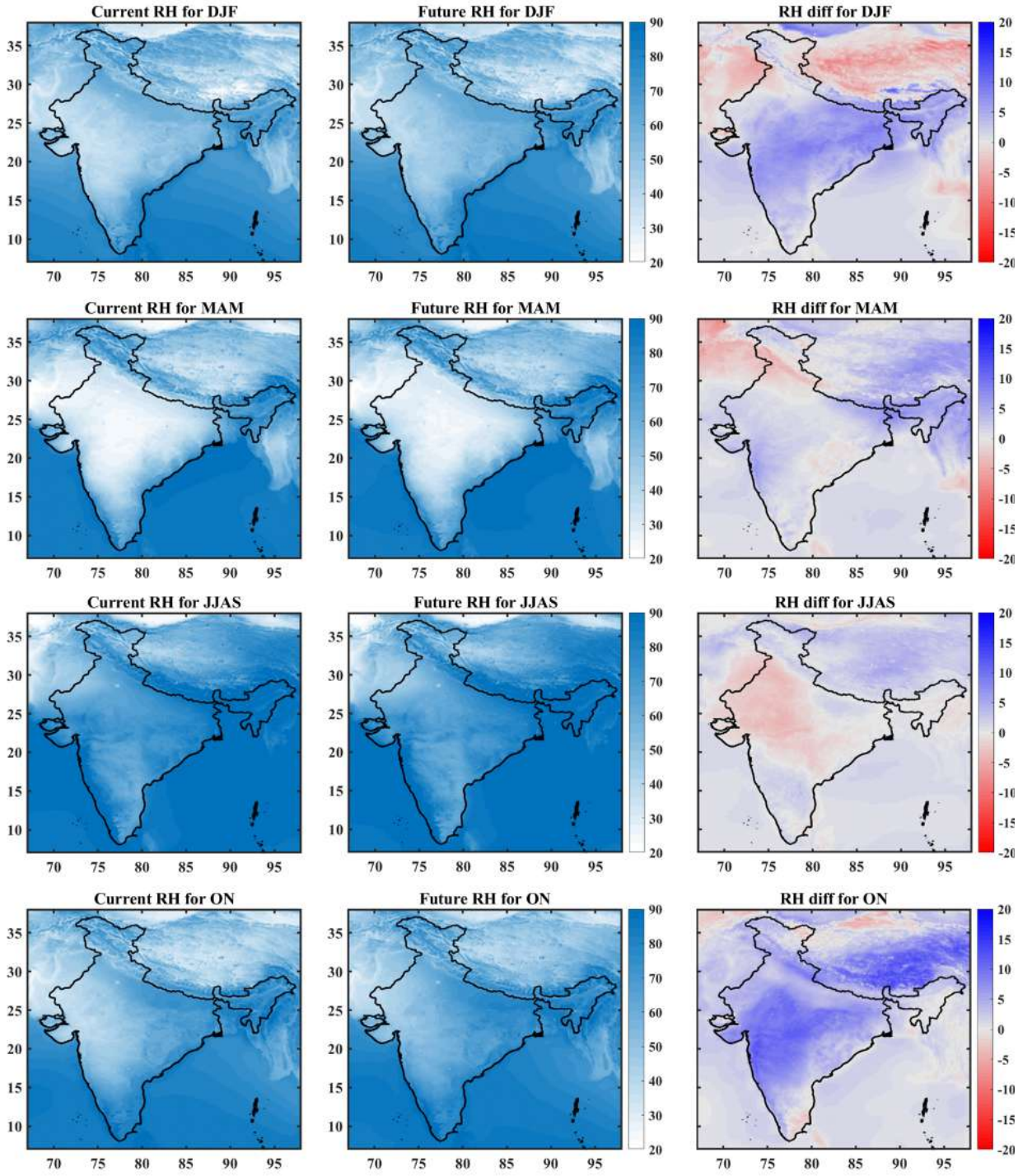

Figure 17: Change in Relative Humidity (%)

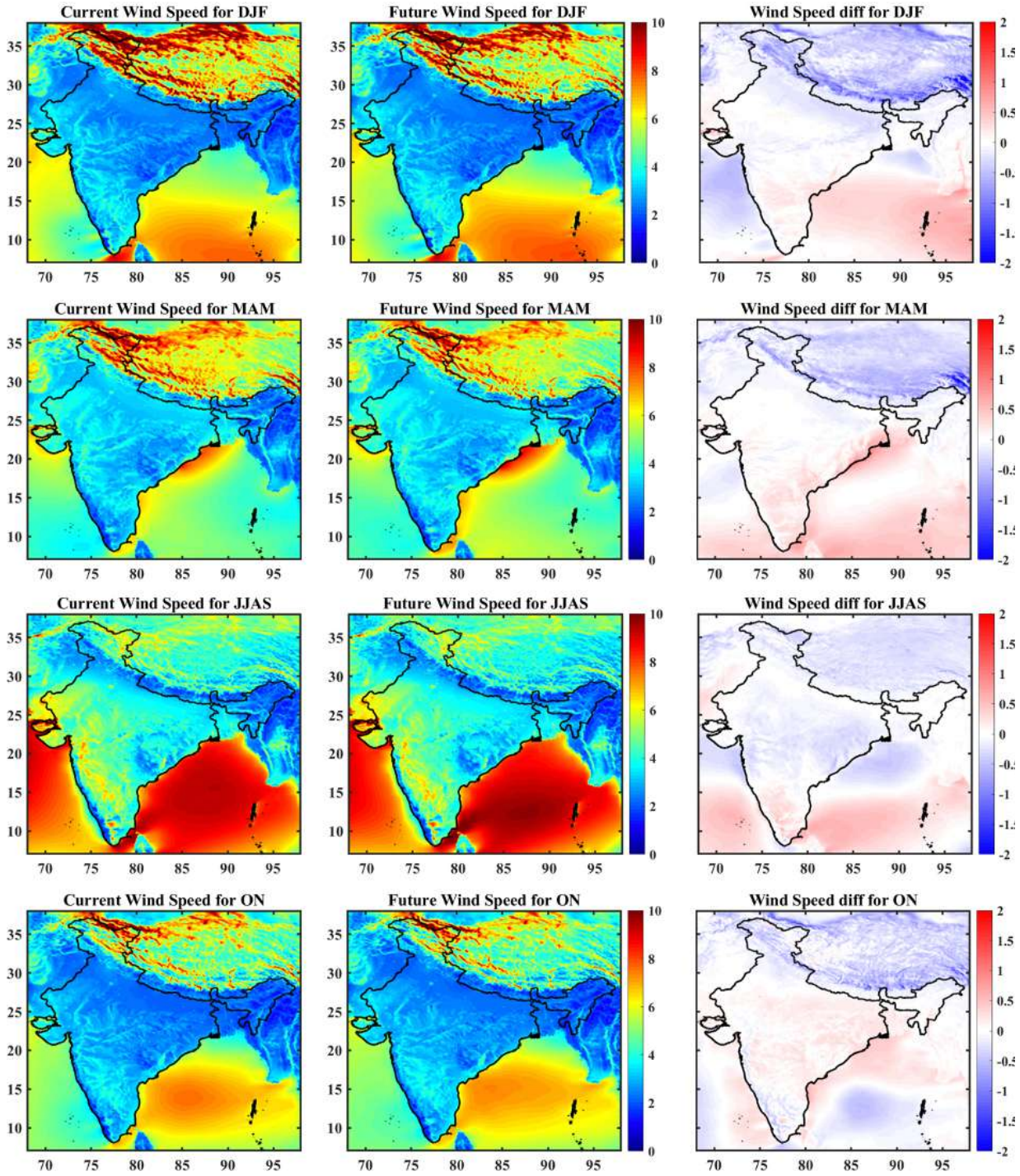

Figure 18: Change in 10m wind speed (m/s)

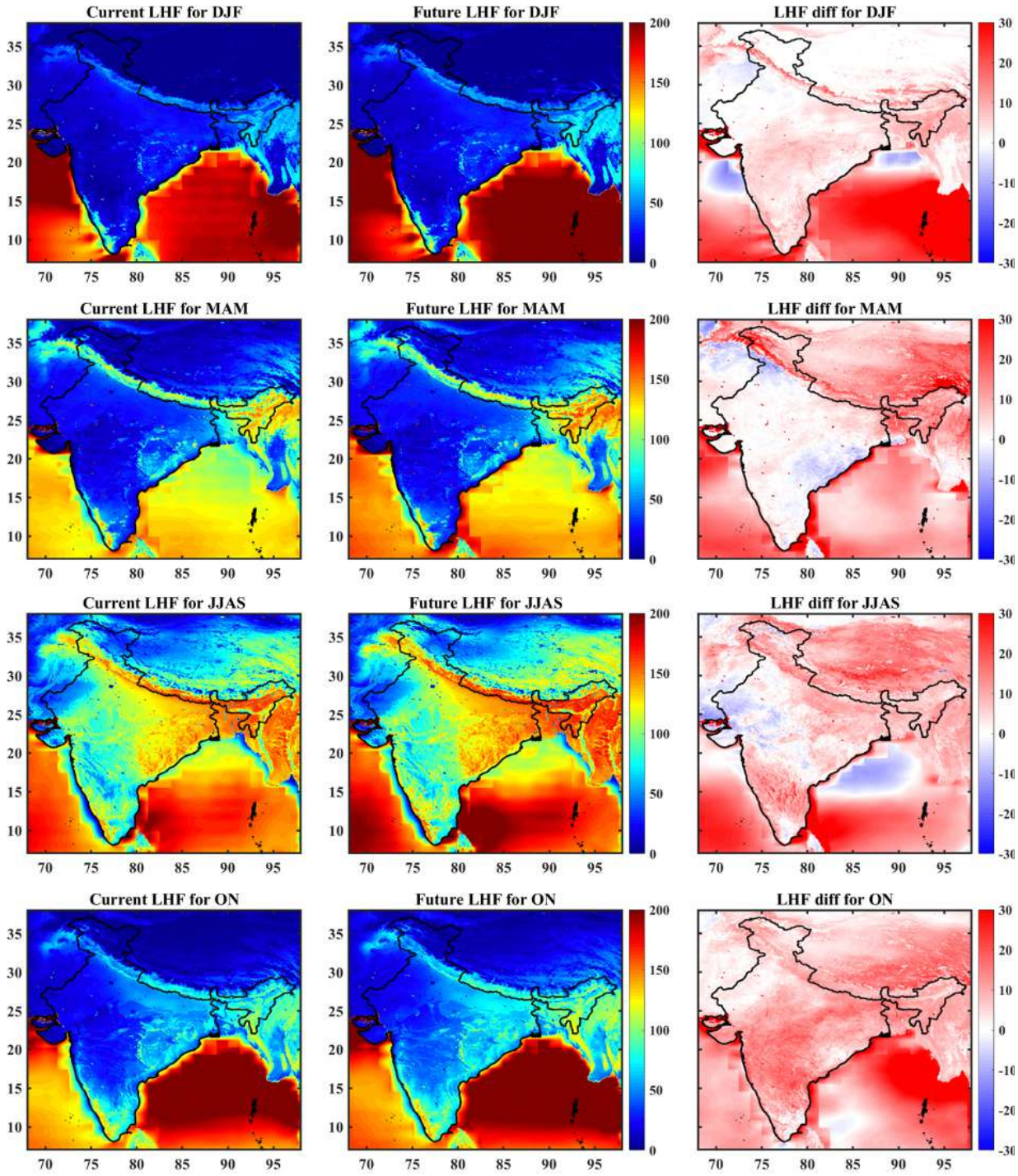

Figure 19: Change in surface latent heat flux (W/m^2)

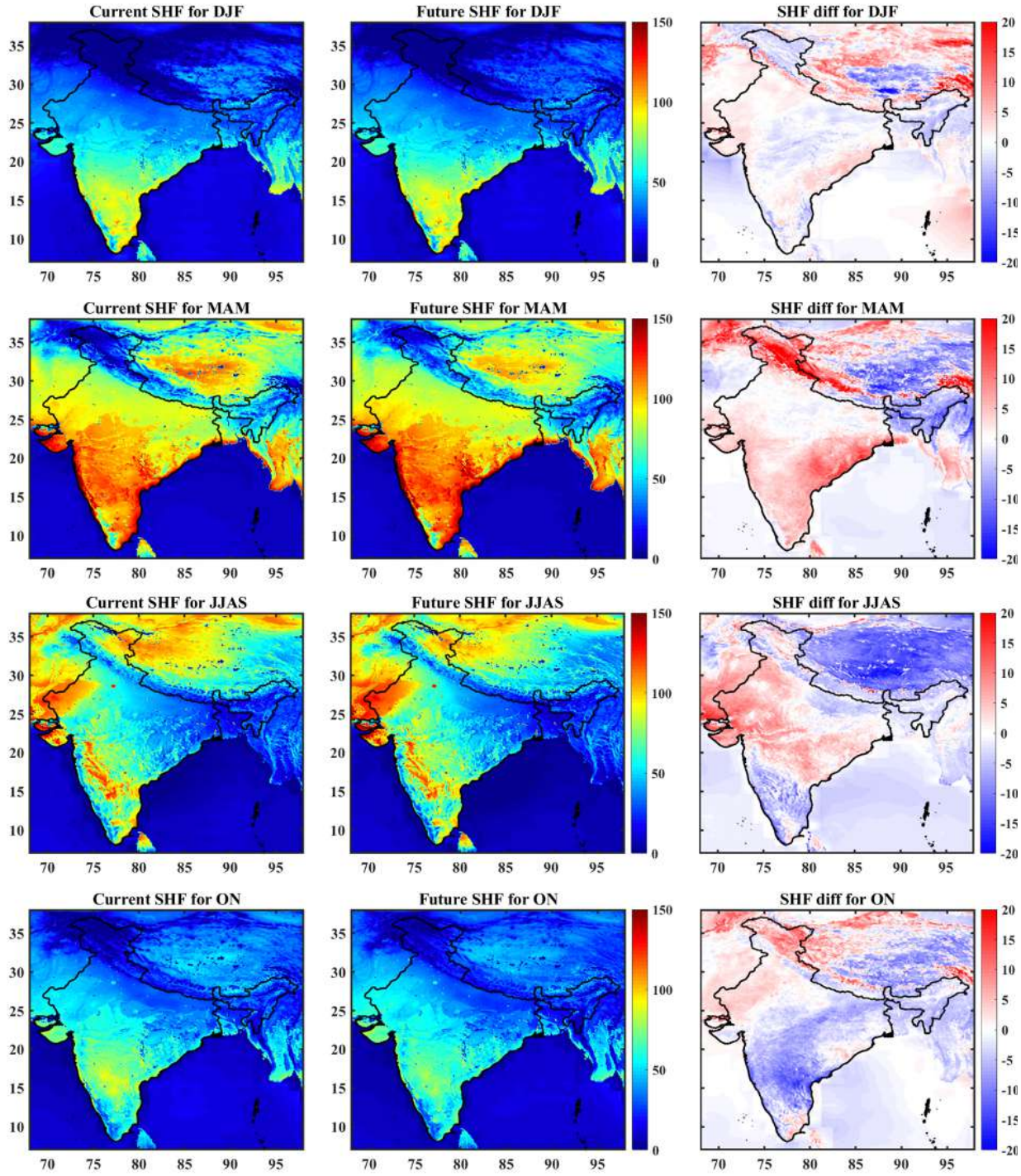

Figure 20: Change in surface sensible heat flux (W/m^2)

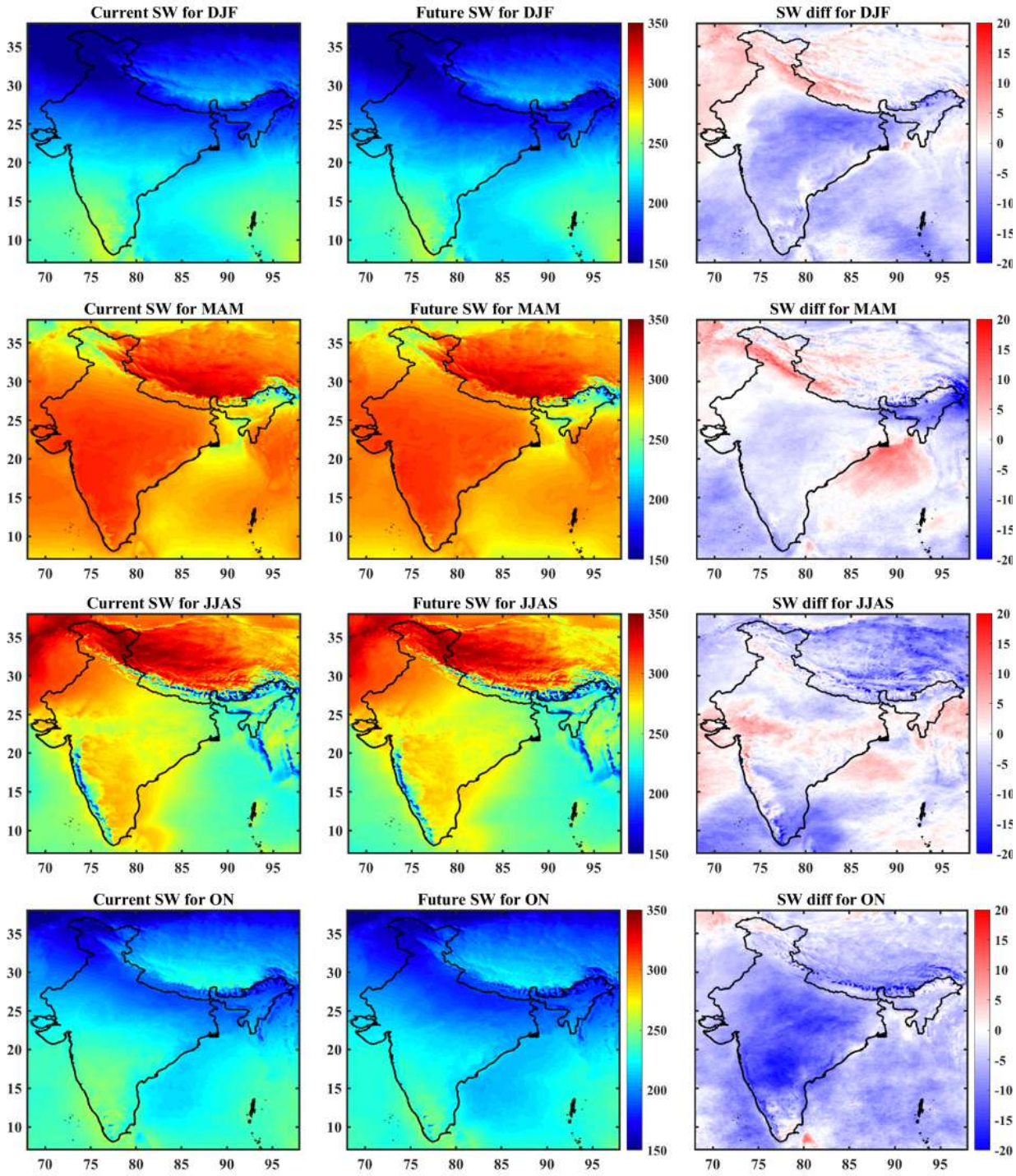

Figure 21: Change in incoming shortwave radiation at the surface (W/m^2)

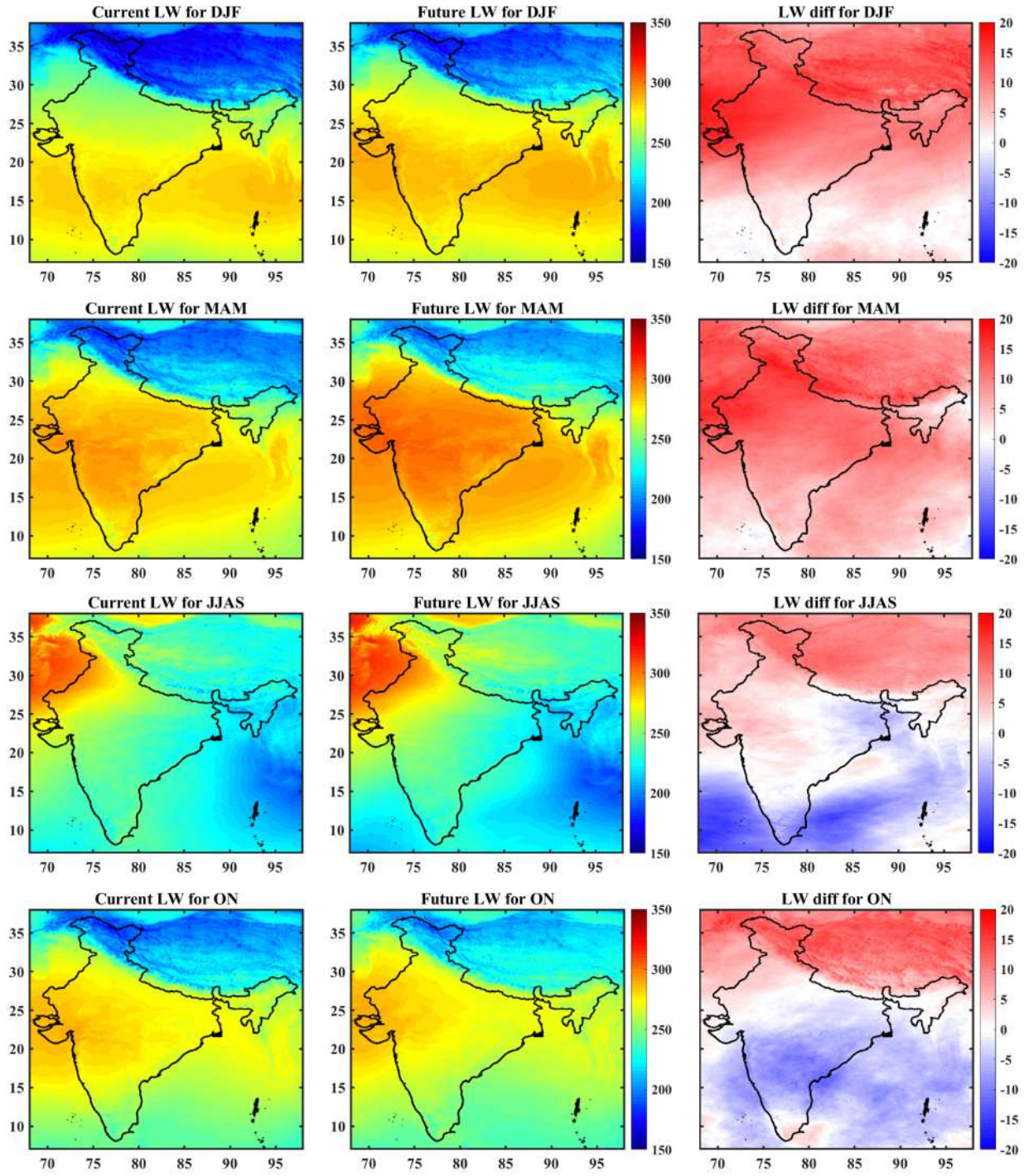

Figure 22: Change in outgoing longwave radiation at the surface (W/m^2)

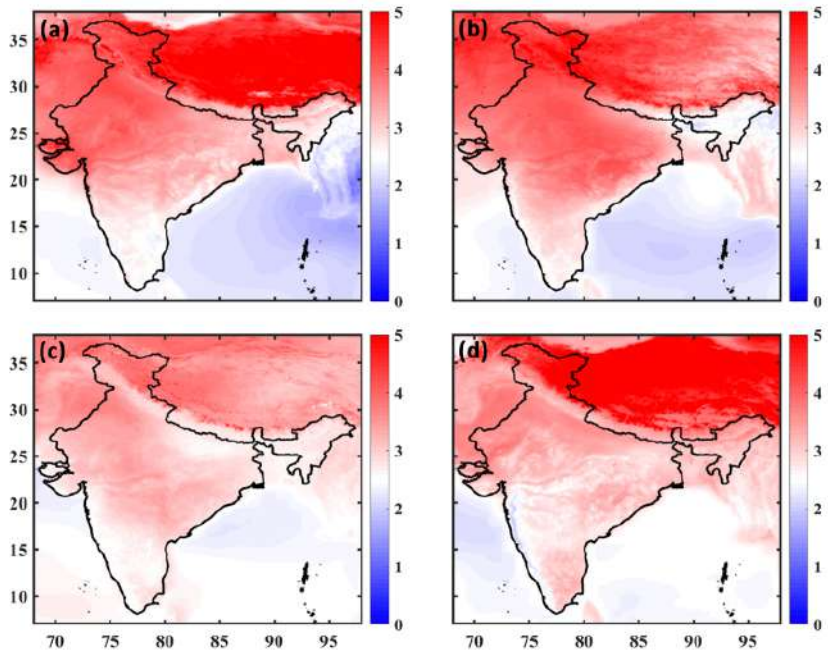

Figure 23: Change in daily mean 2m temperature (°C) for (a) winter, (b) summer, (c) monsoon, and (d) post-monsoon. Only statistically significant (99% level) areas are shown.

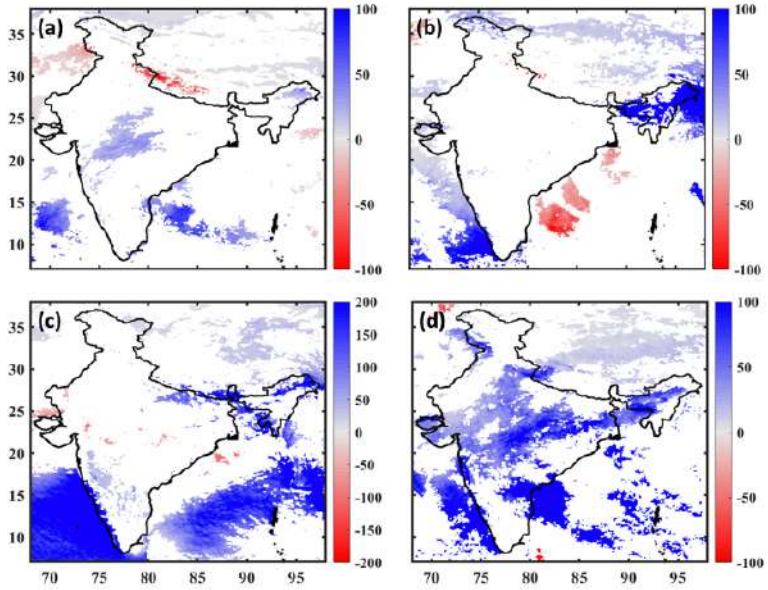

Figure 24: Change in monthly total precipitation (mm) for (a) winter, (b) summer, (c) monsoon, and (d) post-monsoon. Only statistically significant (80% level) areas are shown.

Other meteorological variables show complex patterns that are consistent with changes in temperature and precipitation. The key variables for hydrological applications are incoming shortwave radiation and evaporation or latent heat flux. Incoming shortwave shows a very strong reduction of 20 W/m^2 in the post-monsoon season indicating an increase in cloud cover that is consistent with the increasing rainfall. Evaporation shows a strong increase of 30 W/m^2 in the post-monsoon season due to the increase in precipitation.

3.3.3 Datasets generated

The following datasets are generated from the climate simulations:

1. Current scenario
    1.1. All WRF variables
    1.2. Hourly outputs of 2m temperature, total precipitation (convective + stratiform), 2m relative humidity, 10 m wind speed, surface incoming shortwave radiation, surface outgoing longwave radiation, surface latent heat flux, surface sensible heat flux, soil moisture for 4 soil layers
    1.3. Daily timeseries of daily mean 2m temperature, daily minimum 2m temperature, daily maximum 2m temperature , total precipitation (convective + stratiform), 2m relative humidity, 10 m wind speed, surface incoming shortwave radiation, surface outgoing longwave radiation, surface latent heat flux, surface sensible heat flux, soil moisture for 4 soil layers
    1.4. Daily climatology of 1.3
    1.5. Monthly time series of 1.3
    1.6. Monthly climatology of 1.3
2. Mid-century RCP 8.5 scenario
    2.1. Same as 1.1
    2.2. Same as 1.2
    2.3. Same as 1.3
    2.4. Same as 1.4
    2.5. Same as 1.5
    2.6. Same as 1.6
3. End-century RCP 8.5 scenario
    3.1. Same as 1.1
    3.2. Same as 1.2

3.3. Same as 1.3

3.4. Same as 1.4

3.5. Same as 1.5

3.6. Same as 1.6

3.4 Task 4: District-level downscaled projections

3.4.1 Motivation

The gridded data sets generated in Task 3 will be extremely useful for scientific applications. However, this data is likely to be inaccessible to users beyond the scientific community who may not have the necessary computing equipment, internet connection, software, and the training required to even download and visualise the data let alone analyse it for their purpose. These users will consist of students in local and regional colleges, block and district level planning officials, grassroots organizations, and other stakeholders interested and invested in climate change. To ensure that our work reaches these communities, we generated a dataset of district-scale scenarios of monthly mean climatology of various climate variables in easily accessible MS-Excel format.

3.4.2 Methods

To generate the district- scale data set, we used the ArcGIS software tool. We used a public domain India district shapefile that contains information about the boundaries of all the districts in India in vector format. The gridded data generated in Task 3 are in raster format. Using the district shapefile we converted the variables listed in section 3.3.3 from raster to vector format using interpolation techniques. Then these data were exported to an Excel sheet. The interpolated data was evaluated against the gridded data. Apart from a few limited ~1% interpolations issues, the data was found to be equivalent to the simulated model outputs.

3.4.3 Results

The district-scale can be very useful to understand very local-scale information. For example, Fig. 25 shows the possible change in annual mean temperature for all the districts of India. It is clear that the entire country will experience a warming up to 4 °C by mid-century and up to 4.5 °C by end-century. We can extract the signals for each district individually. For example, Central Delhi local temperatures will

increase by up to 2 °C by mid-century and up to 4 °C across all months with maximum warming occurring during September.

(i) (ii) (iii)

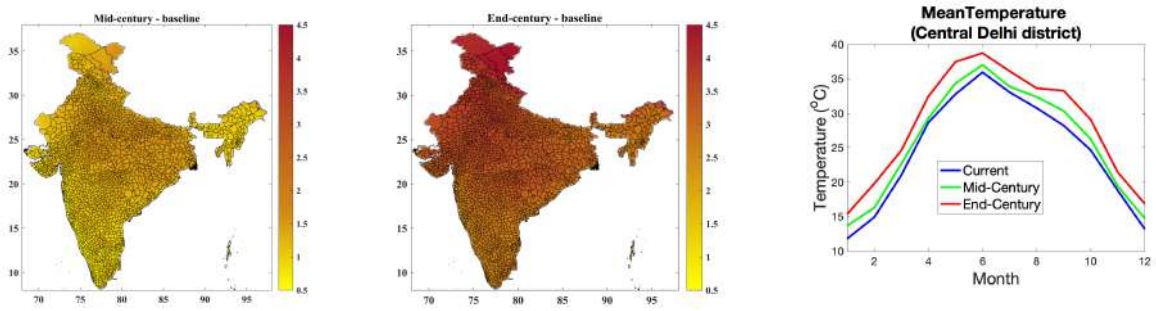

Fig 25: Change in annual mean temperature by (i) mid-century and (ii) end-century; (iii) monthly mean temperatures in Central Delhi

3.5 Task 5: Hydrology model configuration

To demonstrate the applicability of the gridded dataset for hydrologic simulations, we conducted test simulations with the Soil and Water Assessment Tool (SWAT). The SWAT model is developed and supported by the USDA/ARS. It is a physically based watershed-scale continuous time scale model, which operates on a daily time step. The SWAT model can simulate runoff, sediment, nutrients, pesticide, and bacteria transport from agricultural watersheds (R19). The SWAT model delineates a watershed, and sub divides that watershed in to subbasins. In each subbasin, the model creates several hydrologic response units (HRUs) based on specific land cover, soil, and topographic conditions.

Model simulations that are performed at the HRU levels are summarized for the subbasins. Water is routed from HRUs to associated reaches in the SWAT model. SWAT first deposits estimated pollutants within the stream channel system then transport them to the outlet of the watershed. The HRUs provide opportunity to include processes for possible spatial and temporal variations in model input parameters. The hydrologic module of the model quantifies a soil water balance at each time step during the simulation period based on daily precipitation inputs. The SWAT model distinguishes the effects of weather, surface runoff, evapotranspiration, crop growth, nutrient loading, water routing, and the long-term effects of varying agricultural management practices (R20).

SWAT operates on a daily time step and is designed to predict the impact of land use and management on water, sediment, and agricultural chemical yields in ungauged watersheds. The model is process based, computationally efficient, and capable of continuous simulation over long time periods. Major model components include weather, hydrology, soil temperature and properties, plant growth, nutrients, pesticides, bacteria and pathogens, and land management. Major advantage of the SWAT model is that, unlike other conventional conceptual simulation models, it does not require much calibration and therefore can be used on ungauged watersheds.

3.5 Task 6: Hydrology model application over Chambal Basin

The SWAT model was applied over the Chambal Basin. The study domain with the various sub basins and the interventions are given in Fig. 26. For current scenario, the model was driven with the IMD data. For the future scenarios, the model was driven with the downscaled CESM data generated in Task 3.

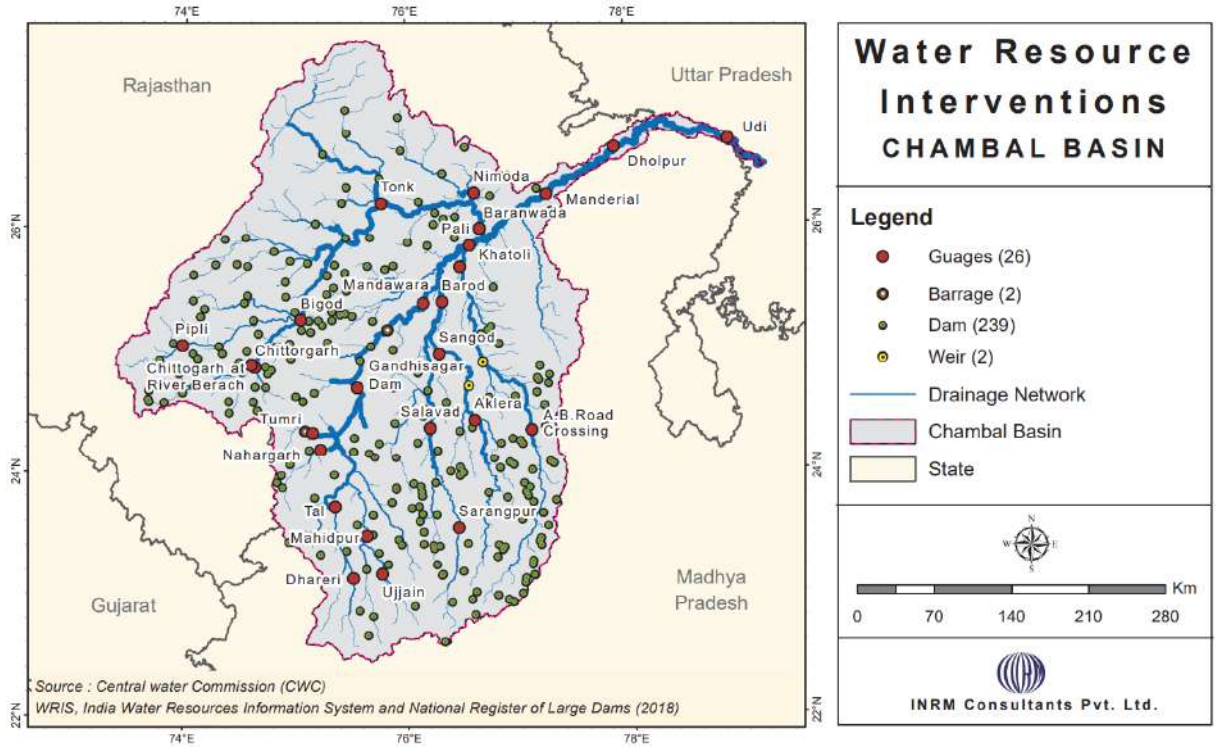

Figure 26: Chambal basin as represented in the SWAT model

The simulated long term monthly flow is shown in Figure 27. The annual average water balance components show that there is considerable heterogeneity in precipitation across the basin. The surface

run-off also varies due to the complex topography of the region. The baseflow is low due to high evaporative and anthropogenic losses. However, the baseflow of the Chambal basin will increase in the

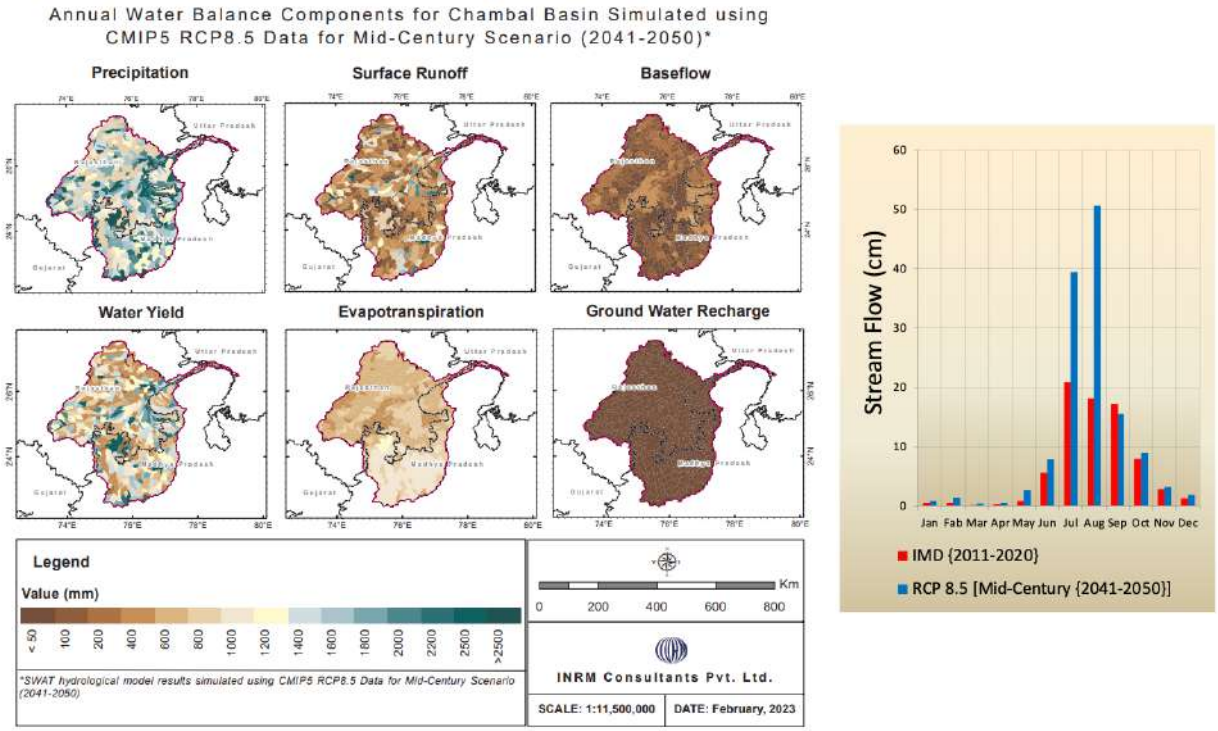

Fig 27: (Left) Mid-century annual water balance components and (Right) streamflow for the Chambal Basin.

future climate scenario. The increase in the flow in the late monsoon season is quite large indicating the need for water management to prevent possible flooding.

4. Deliverables

3.3.1 Current and future climate data:

The following datasets are archived in the public domain:

i. The gridded monthly time series and monthly climatological mean data are archived in NetCDF format and available for download at https://doi.org/10.5281/zenodo.4899405. Data citation: Baidya Roy, Somnath. (2021). Bias-corrected CMIP5 CESM projections over India dynamically downscaled to 10 km resolution by WRF [Data set]. Zenodo. https://doi.org/10.5281/zenodo.4899405

ii. The daily time series, monthly time series, and monthly climatological mean data are archived in NetCDF format and available for download at https://www.wdc-climate.de/ui/entry?acronym=WRF10km_wbc_C5_forc_oIndia. Data citation: Barik, Anasuya; Sahoo, Sanjeeb Kumar; Kumari, Sarita; Baidya Roy, Somnath (2021). 10 km gridded hydrometeorological dataset developed by dynamical downscaling of the bias-corrected CMIP5 CESM RCP8.5 projections over India for current (2006-2015) and future (2091-2100) periods using WRF. World Data Center for Climate (WDCC) at DKRZ. https://doi.org/10.26050/WDCC/WRF10km_wbc_C5_forc_oIndia

iii. The district-scale monthly climatology data are archived in Excel format and available at https://zenodo.org/record/6546582#.Y-dxW-xBz6A. Data citation: Sahoo, Sanjeeb Kumar, Bhat, Nagaraj, Barik, Anasuya, & Baidya Roy, Somnath. (2022). All-India district-scale climate projections for current (2006-2015), mid-century (2041-50), and end-century (2091-2100) periods [Data set]. Zenodo. https://doi.org/10.5281/zenodo.6546582

3.3.2 Hydrology data

The basin scale hydrology data are archived on IIT Delhi servers and are available on request.

5. References:

R1: Yuan Qiu, Qi Hu, Chi Zhang. 2017. WRF simulation and downscaling of local climate in Central Asia. Int. J. Climatol. 37: 513 – 528.

R2: U. Heikkilä, A. Sandvik, A. Sorteberg. 2011. Dynamical downscaling of ERA-40 in complex terrain using the WRF regional climate model. Clim. Dynamics, 37:1551–1564 DOI 10.1007/s00382-010-0928-6.

R3: Xuguang Sun1, Ming Xue, Jerald Brotzge, Renee A. McPherson, Xiao-Ming Hu, and Xiu-Qun Yang. 2016. An evaluation of dynamical downscaling of Central Plains summer precipitation using a WRF-basedregional climate model at a convection-permitting 4 km resolution. J. Geophys. Res. Atmos.121, 13,801–13,825, doi:10.1002/2016JD024796.

R4: Tomi Afrizal and Chinnawat Surussavadee. 2018. High-Resolution Climate Simulations in the Tropics with Complex Terrain Employing the CESM/WRF Model Advances in Meteorology. Article ID 5707819 https://doi.org/10.1155/2018/5707819

R5: Liang Chen, Zhuguo Ma, Zhenhua Li, Lin Wu, Jason Flemke & Yanping Li (2018) Dynamical Downscaling of Temperature and Precipitation Extremes in China under Current and Future Climates, Atmosphere-Ocean, 56:1, 55-70, DOI: 10.1080/07055900.2017.1422691

R6: He, J.; Lu, S.; Yu, Y.; Gong, S.; Zhao, S.; Zhou, C. Numerical Simulation Study of Winter Pollutant Transport Characteristics over Lanzhou City, Northwest China. *Atmosphere* 2018, *9*, 382.

R7: Tran Anh, Q., Taniguchi, K. Coupling dynamical and statistical downscaling for high-resolution rainfall forecasting: case study of the Red River Delta, Vietnam. *Prog Earth Planet Sci* 5, 28 (2018) doi:10.1186/s40645-018-0185-6

R8: Wootten, A., J.H. Bowden, R. Boyles, and A. Terando, 2016: The Sensitivity of WRF Downscaled Precipitation in Puerto Rico to Cumulus Parameterization and Interior Grid Nudging. *J. Appl. Meteor. Climatol.,* 55, 2263–2281, https://doi.org/10.1175/JAMC-D-16-0121.1

R9: Fonseca, R. & Martín-Torres, High-resolution dynamical downscaling of re-analysis data over the Kerguelen Islands using the WRF model, J. Theor Appl Climatol (2019) 135: 1259. https://doi.org/10.1007/s00704-018-2438-0

R10: C. V. Srinivas D. Hariprasad D. V. Bhaskar Rao Y. Anjaneyulu R. Baskaran B. Venkatraman, Simulation of the Indian summer monsoon regional climate using advanced research WRF model, Int. J. Climatology, 33, 2013, 1195-1210.

R11: Ila Chawla, Krishna K. Osuri, Pradeep P. Mujumdar, and Dev Niyogi Assessment of the Weather Research and Forecasting (WRF) model for simulation of extreme rainfall events in the upper Ganga Basin . Hydrol. Earth Syst. Sci., 22, 1095–1117, 2018, https://doi.org/10.5194/hess-22-1095-2018

R12: Alsarraf, Hussain & Broeke, Matthew. (2015). Using the WRF Regional Climate Model to Simulate Future Summertime Wind Speed Changes over the Arabian Peninsula. Journal of Climatology & Weather Forecasting. 03. 10.4172/2332-2594.1000144.

R13: Ratna, S. B., Ratnam, J. V., Behera, S. K., Tangang @ Tajudin Mahmud, F., & Yamagata, T. (2017). Validation of the WRF regional climate model over the subregions of Southeast Asia: Climatology and interannual variability. *Climate Research*, *71*(3), 263-280. https://doi.org/10.3354/cr01445

R14: Zhou, Y.; Mu, Z. Impact of Different Reanalysis Data and Parameterization Schemes on WRF Dynamic Downscaling in the Ili Region. *Water* 2018, *10*, 1729.

R15: Andrys, J., T.J. Lyons, and J. Kala, 2015: Multidecadal Evaluation of WRF Downscaling Capabilities over Western Australia in Simulating Rainfall and Temperature Extremes. *J. Appl. Meteor. Climatol.,* 54, 370–394, https://doi.org/10.1175/JAMC-D-14-0212.1

R16: Mahoney, K., M. Alexander, J.D. Scott, and J. Barsugli, 2013: High-Resolution Downscaled Simulations of Warm-Season Extreme Precipitation Events in the Colorado Front Range under Past and Future Climates. *J. Climate,* 26, 8671–8689, https://doi.org/10.1175/JCLI-D-12-00744.1

R17: Tariku, T.B., Gan, T.Y. Sensitivity of the weather research and forecasting model to parameterization schemes for regional climate of Nile River Basin. *Clim Dyn* 50, 4231–4247 (2018) doi:10.1007/s00382-017-3870-z

R18: Caldwell, P., Chin, HN.S., Bader, D.C. et al. Evaluation of a WRF dynamical downscaling simulation over California, Climatic Change (2009) 95: 499. https://doi.org/10.1007/s10584-009-9583-5

R19: Arnold J. G., Srinivasan R., Muttiah R. S., and Williams J. R. 1998. Large area hydrologic modeling and assessment, Part I: model development. Journal of American Water Resources Association, 34(1): 73-89.

R20: Neitsch S. L., Arnold J. G., Kiniry J. R., and Williams J. R. 2005. Soil and water assessment tool (SWAT), theoretical documentation, Blackland research center, grassland, soil and water research laboratory, agricultural research service: Temple, TX.